ACS SENSORS

Review

Cite This: ACS Sens. 2018, 3, 2025−2044

pubs.acs.org/acssensors

Stress Biomarkers in Biological Fluids and Their Point-of-Use Detection

Andrew J. Steckl* and Prajokta Ray

Nanoelectronics Laboratory, University of Cincinnati, Cincinnati, Ohio 45221-0030, United States

Supporting Information

ABSTRACT: Hormones produced by glands in the endocrine system and neurotransmitters produced by the nervous system control many bodily functions. The concentrations of these molecules in the body are an indication of its state, hence the use of the term *biomarker*. Excess concentrations of biomarkers, such as cortisol, serotonin, epinephrine, and dopamine, are released by the body in response to a variety of conditions, for example, emotional state (euphoria, stress) and disease. The development of simple, low-cost modalities for point-of-use (PoU) measurements of biomarkers levels in various bodily fluids (blood, urine, sweat, saliva) as opposed to conventional hospital or lab settings is receiving increasing attention. This paper starts with a review of the basic properties of 12 primary stress-induced biomarkers: origin in the body (i.e., if they are produced as hormones, neurotransmitters, or both), chemical composition, molecular weight (small/medium size molecules and polymers, ranging from ∼100 Da to ∼100 kDa), and hydro- or lipophilic nature. Next is presented a detailed review of the published literature regarding the concentration of these biomarkers found in several bodily fluids that can serve as the medium for determination of the condition of the subject: blood, urine, saliva, sweat, and, to a lesser degree, interstitial tissue fluid. The concentration of various biomarkers in most fluids covers a range of 5−6 orders of magnitude, from hundreds of nanograms per milliliter (∼1 μM) down to a few picograms per milliliter (sub-1 pM). Mechanisms and materials for point-of-use biomarker sensors are summarized, and key properties are reviewed. Next, selected methods for detecting these biomarkers are reviewed, including antibody- and aptamer-based colorimetric assays and electrochemical and optical detection. Illustrative examples from the literature are discussed for each key sensor approach. Finally, the review outlines key challenges of the field and provides a look ahead to future prospects.

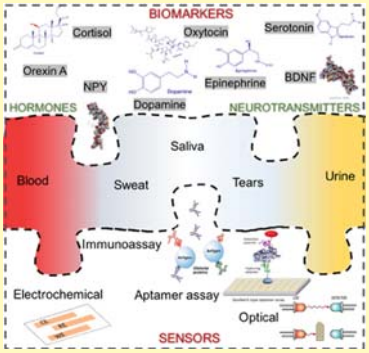

KEYWORDS: *stress biomarkers, blood, sweat, urine, saliva, sensors, point-of-use*

In the world of mechanics, the relationship between an applied force (stress) on an object results in a certain amount of deformation (strain) depending on its materials properties. In the biological world, stress has more complex results. For example, plants can be put under stress by environmental factors (such as extremes of temperature or moisture) and/or attack by herbivores, insects, or pathogens.[1] The stress triggers specific biological responses in plants designed to counteract the effect (for example, by reducing water elimination during drought conditions) or to repel the attackers (through the release of chemicals).[1] In animals and, in particular, in sentient human beings, the effect of stress is made more complex yet by the ability to recognize the condition.[2] This cognitive aspect can lead to an increase in the effect of stress or its reduction depending on the specific stressor and the emotional and physical makeup of the individual under stress.[3] Stress can take many forms,[4] from short-term extreme situations (such as the fight-or-flight response caused by a potential personal attack) to long-term chronic stress of a lower level (such as caused by health issues).[5]

Monitoring the stress level on a routine (and sometimes continuous) basis is becoming very important for many groups, including those in stressful occupations (armed forces personnel, police, firefighters, emergency personnel), athletes, and individuals with certain medical conditions or wanting to improve their overall health status. To monitor stress levels while performing regular duties or activities in the home requires a sensing methodology that can produce relatively simple, compact, and low-cost instruments. Since many individuals that would be interested in stress monitoring are fundamentally healthy, the label point-of-use (PoU) device is more appropriate than the commonly used point-of-care (PoC) descriptor.

This review focuses on properties of stress-related biomarkers and associated detection methods suitable for PoU situations. A general definition of biomarkers has been established[6] by the American National Institutes of Health (NIH) and the Food and Drug Administration (FDA) as "A defined characteristic that is measured as an indicator of normal biological processes, pathogenic processes, or responses to an exposure or intervention, including therapeutic interventions. Molecular, histologic, radiographic, or physiologic characteristics are types

Received: July 27, 2018
Accepted: September 28, 2018
Published: September 28, 2018

DOI: 10.1021/acssensors.8b00726
ACS Sens. 2018, 3, 2025−2044

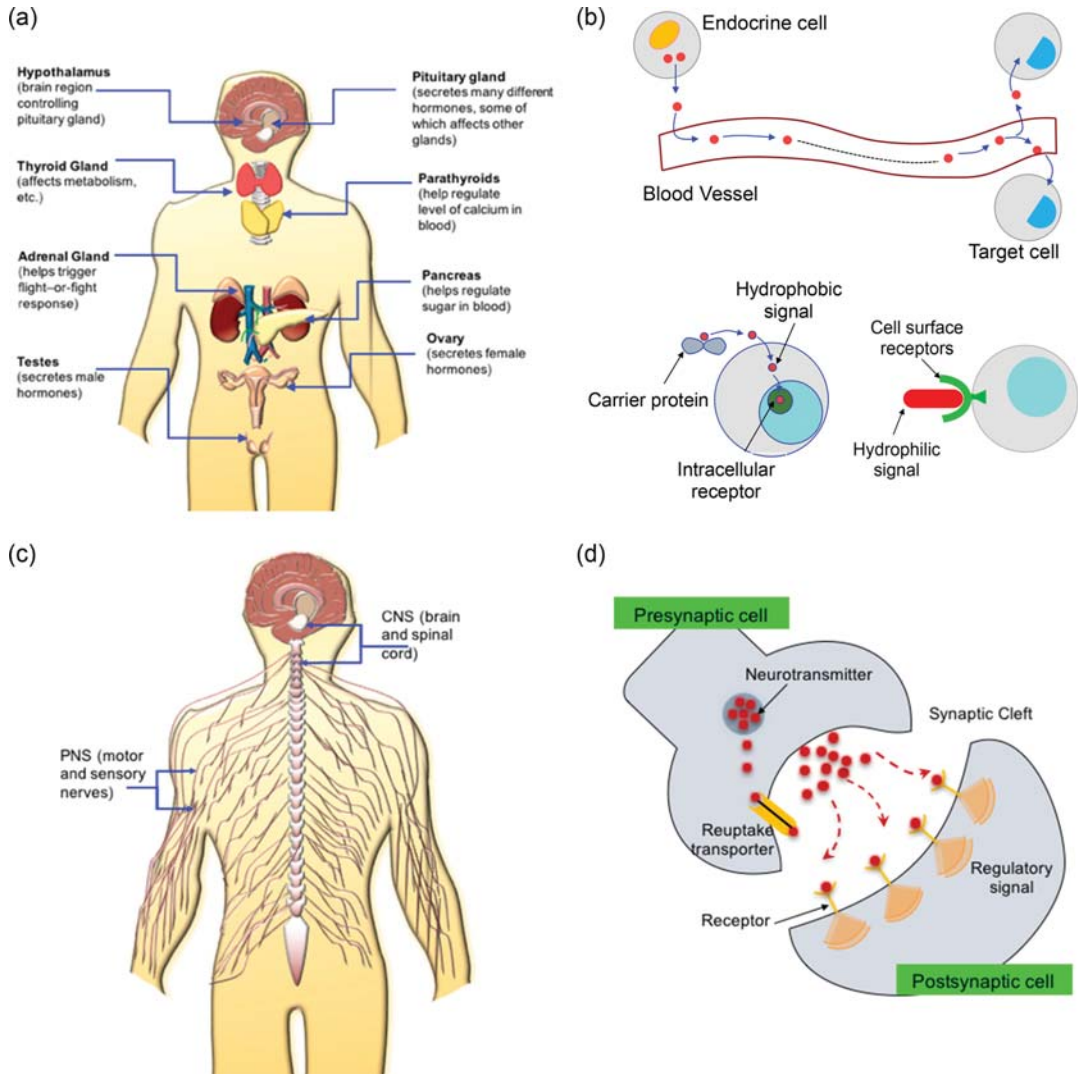

Figure 1. Endocrine and nervous systems control body functions using signals carried by hormones and neurotransmitters.

of biomarkers." For the purpose of this review, a much narrower definition is used, namely biomarkers that are molecules present in biological fluids and whose concentrations vary with the stress level of the individual. In the review, a series of biomarkers are considered in detail in the following bodily fluids: blood (or plasma), saliva, sweat, urine, and tissue interstitial fluid. The paper contains a review of the key properties of stress biomarker molecules (such as origin, molecular weight, hydrophilic/phobic) and a compendium of their concentrations reported in biofluids. Since the review is intended to provide information and hopefully useful guidance to the sensor community, an overview of detection mechanisms and examples of biosensors is also provided, along with an introduction to the origin and nature of stress biomarkers in the human body.

STRESS BIOMARKERS AND SELECTED PROPERTIES AND CONCENTRATIONS

The body responds to stress by the release of certain molecules which play key roles in mediating its effect.[7] This includes hormones released by the endocrine (glandular) system[8] and neurotransmitters released by the nervous system.[9,10] The endocrine system consists of multiple glands which control, regulate, or trigger many functions in the body. The endocrine system and the nervous system interact in order to maintain a stable equilibrium ("homeostasis") in the body.[11] A much-simplified illustration[12] of the endocrine system is shown in Figure 1a. For example, the thyroid gland controls the metabolism[13] while adrenal glands trigger the "fight-or-flight" response to a stressful situation.[14] This control function is accomplished by the generation of molecules (hormones) that communicate the signal from the gland to the target cell in selected tissues and organs.[15] Hormones are typically released into the bloodstream, where they travel until they reach their target (Figure 1b). Certain hormones are hydrophilic and can travel readily in blood vessels.[16] When they reach the cell target, hydrophilic hormones impart their "signal" by attaching to cell surface receptors.[17] Hydrophobic hormones travel in the bloodstream with the aid of carrier proteins and are injected into the cell nucleus[18] where they attach to intracellular (nuclear) receptors.[19,20] Since this review is focused on biomarkers related to stress, the interaction of biomarkers with nuclear receptors that are primarily involved in gene regulation[21] via transcription factors, while very important, are not discussed here.

DOI: 10.1021/acssensors.8b00726
ACS Sens. 2018, 3, 2025−2044

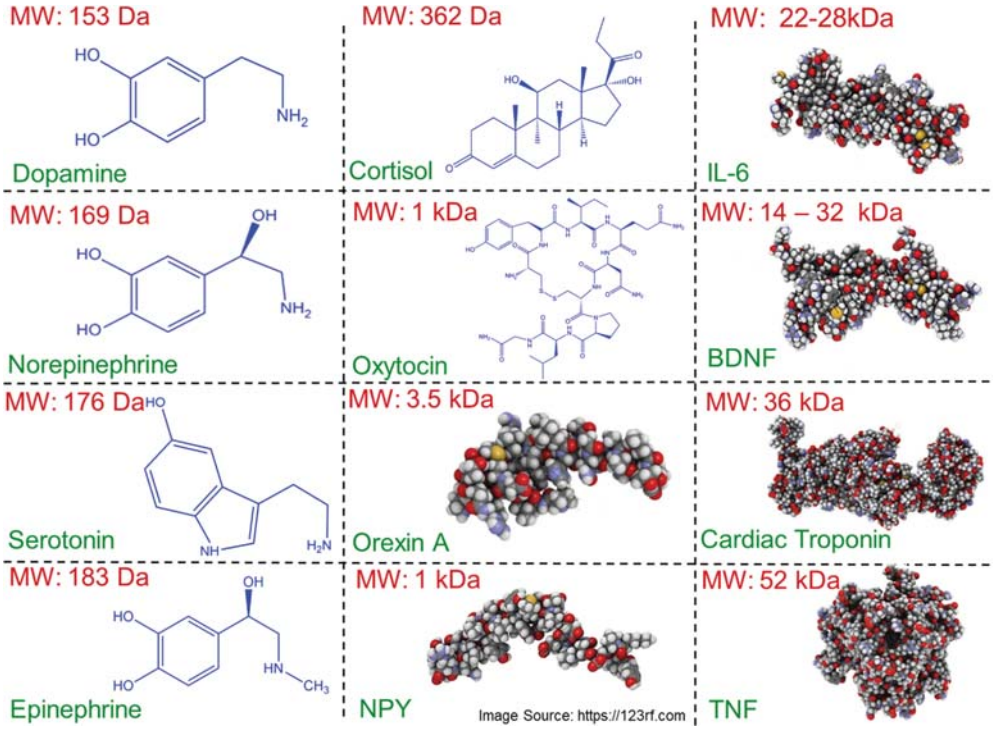

Figure 2. Molecular structure of stress biomarkers in bodily fluids.

The nervous system is illustrated in Figure 1c, also in a much-simplified fashion. It consists of the central nervous system (the brain and the spinal cord) and the peripheral nervous system (motor and sensory nerves).[22] Neurotransmitters are molecules that act as chemical messengers[23] which transmit nerve signals from a specific originating nerve cell (neuron) to a specific target, such another neuron, muscle, or gland cell.[24] As illustrated in Figure 1d, the neural signal ("action potential") travels along the neuron body ("axon") until it reaches a synapse, the gap between the axon terminal of one neuron and the receiving terminal ("dendrite") of another neuron.[25] Signal transmission across the synapse occurs as the axon action potential causes neurotransmitters to be released in the presynaptic neuron that can then bind to receptors in the postsynaptic membrane where it can release a secondary signal.[26] Among other functions, the nervous system controls involuntary body operations, such as those of the heart, lungs, and stomach, through the neurotransmission process. Other neurotransmitters can affect mood and response to stress.[27] Excitatory neurotransmitters stimulate activity, while inhibitory neurotransmitters control overacting stimulation and produce a balanced mood.[28]

As illustrated in Figure 2, biomarker structures include molecules of various sizes and molecular weights, ranging from small molecules, such as the catecholamines (dopamine, epinephrine, etc.), to large protein molecules, such as BDNF and IL-6. While in this review we have focused on hormone and neurotransmitter biomarkers, we do want to point out that there are other biomarker types (such as enzymes, metabolic biomarkers) that can be related to stress and human performance and have been detected through PoU platforms. One such example is the enzyme salivary α-amylase which is a digestive enzyme and an indicator for chronic (rather than short-term) stress conditions and is found in high concentrations in saliva.[29]

One of the goals of this literature survey is to provide an overview of key stress biomarkers and of their concentrations that can serve as a roadmap for future development of sensors for specific markers in selected biological fluids. Properties of these biomarker molecules are summarized in Table 1. Figure 3 plots the results of the literature review for selected biomarker concentrations (under healthy physiological conditions) in key body fluids as a function of their molecular weight: (a) whole blood; (b) urine; (c) saliva; (d) sweat; and (e) interstitial fluid in tissues.

A few general observations can be made from Figure 3:

- biomarker concentrations range over 6 orders of magnitude, from pg/mL to μg/mL;
- biomarkers with the highest concentrations are *usually* small molecules;
- biomarker concentration tends to decrease with molecular weight; this decrease is even more pronounced in terms of molar concentration;
- most common biomarkers are serotonin (highest in whole blood), dopamine (highest in urine), and cortisol (highest in sweat, close second in blood); α-amylase has a very high concentration in saliva ($\sim$ 1 mg/mL).

In Figure 3, the biomarkers have been color coded based on their solubility properties: red, lipophilic; blue, hydrophilic; green, amphiphilic. For many detection techniques, the biomarker molecular weight, physical size, and solubility are key factors in the specifics of the measurement.[30] For example, in immunochemical assays based on antibody–antigen interaction, the analyte target molecular weight, size, and structure are key factors in determining the type of assay to be developed. The *sandwich* assay (antibody–analyte–antibody) is utilized for large analyte molecules that have multiple antibody binding sites (epitopes), whereas for small analyte molecules the *competitive* assay (antibody–analyte) approach is generally used.[31,32] The solubility properties of the biomarkers are the result of their molecular structure: polar terminal groups

DOI: 10.1021/acssensors.8b00726
ACS Sens. 2018, 3, 2025–2044

Table 1. Properties of Stress Biomarkers[a]

biomarker	origin and transport	molecule type, weight	healthy individuals, normal conditions		related health condition(s)
			wt/mL	molarity	
α-amylase (α-1,4-α-D-glucan 4-glucanohhydrolase enzyme)	origin, neuronal stimuli to epithelial acinar cells of parotid salivary gland	protein, 50−55 kDa, lipophillic	saliva, 0.6−2.6 mg/mL (90−250 U/mL)	saliva, 11−48 μM	acute psychological stress, higher concn release after heightened adrenergic stimuli
BDNF (brain derived neutropic factor)	origin, sympathetic nerve terminals	protein, 14−32 kDa, lipophilic	serum, 3.0−43 ng/mL; plasma, median, 0.1 ng/mL; saliva, 0.067−2.74 ng/mL	serum, 0.1−2 nM; plasma, 4 pM; saliva, 0.003−0.2 nM	neuropsychiatric, depression, schizophrenia
cortisol	origin, zona fasciculata of adrenal cortex of adrenal gland; circulation, blood	glucocorticoid; $C_{21}H_{30}O_5$, 362 Da; lipophilic	blood,50−230 (am), 30−160 ng/mL (pm); sweat, 8−142 ng/mL; urine, 10−100 ng/mL; saliva, 1−1.6 ng/mL	blood, 0.1−0.8 μM; sweat, 0.02−0.4 μM; urine, 0.03−0.3 μM; saliva, 2.8−4.4 nM	stress hormone; acute stress, low-blood glucose; obesity, depression, diabetes
CTT (cardiac troponin T)	origin, cardiac muscle; serum, primary abundance in cardiac muscle enzyme	protein, 36 kDa, hydrophobic core	plasma, 1−8 pg/mL; body fluids, under study	plasma, 0.02−0.2 pM; body fluids: under study	key biomaker for heart disorder (increased troponin in plasma)
dopamine	source, dopaminergic neuron; origin, brain substantia nigra (abundance production)	neurotransmitter, hormone; $C_8H_{11}NO_2$, 153 Da; lipophilic	plasma, 0−37 pg/mL; urine, 52−480 ng/mL; sweat, under study	blood, 0−0.25 nM; urine, 0.3−3 μM	feelings of happiness (natural, induced)
epinephrine (aka adrenaline)	source, adrenal medulla (primary), sympathetic neuron (secondary)	amino acid derived hormone; $C_9H_{13}NO_3$, 183 Da; hydrophilic	blood, 0−0.028 ng/mL; urine, 0−20 ng/mL; sweat, under study	blood, 0−0.15 nM; urine, 0−0.1 μM; sweat, under study	drives automatic nervous system emergency response (flight or fight); increases heart rate, blood pressure
IL-6 (interleukin-6)	origin, cellular inflammation at site; transport, plasma	cytokine; 22−28 kDa; amphiphilic	plasma, 0−4.3 pg/mL; sweat, 7−16 pg/mL; saliva, 2.5 pg/mL; urine, 20−30 pg/mL	plasma, 0−0.16 pM; sweat, 0.3−0.6 pM; saliva, 0.1 pM; urine, 0.8−1.2 pM	secreted by T-cells to stimulate immune response; inflammatory, auto immune process; stimulator of acute phase protein inflammation at site
norepinephrine	source, sympathetic nerve fibers (primary), adrenal gland (secondary); as hormone, released in blood through adrenal gland	neurotransmitter and hormone; $C_8H_{11}NO_3$, 169 Da; hydrophilic	blood, 0−0.0.6 ng/mL; urine, 15−80 ng/mL; other, under study	blood, 0−0.3.5 nM; urine, 0.09−0.5 μM; other, under study	stress hormone (chemically similar to dopamine); high glucose, increased heart rate; anxiety, high blood pressure
NPY (neuropeptide Y)	origin, adreno-medullary nervous system; circulation: blood	polypetide, 36-amino acid; $C_{190}H_{287}N_{55}O_{57}$, 4.3 kDa; lipophilic	plasma, 0.6−2.6 pg/mL; sweat, 0.8−2.9 pg/mL; saliva, 0.04−0.05 ng/mL	blood, 0.14−0.6 pM; urine, 0.1−0.7 pM; saliva, 10−12 pM	depression, anxiety, PTSD; food intake; stress response, cardiovascular function
orexin A	origin, lateral hypothalamus; diffused into blood	33-amino acid; $C_{152}H_{243}N_{47}O_{44}S_4$, 3.5 kDa; lipophilic	plasma, 0.3 ng/mL; blood fluids, under study	plasma, 83 pM; blood fluids, under study	controls consciousness; sleep disorder, appetite; affects histamine, dopamine, NPY
oxytocin	origin, hypothalmus neurosecretory cells; stored: posterior pituitary gland (released to bloodstream)	$C_{43}H_{56}N_{12}O_{12}S_2$, 1 kDa; hydrophilic	plasma, 0.016−0.07 ng/mL; blood fluids, under study	plasma, 16−70 pM; blood fluids, under study	social bonding, emotion maternity, child birth; oxytocin has anxiolytic effect; oxytocin administered to initiate labor during childbirth
serotonin	source, serotonergic neuron; origin, raphe nuclei of brain	neurotransmitter; $C_{10}H_{12}NO_2O$, 176 Da; amphiphilic	blood, 101−283 ng/mL; urine, 5−13 ng/24 h	blood, 0.6−2 μM; urine, 0.03−0.13 μM	mood regulation, appetite; antidepressant
TNF α	origin, cell inflammation at site; transport, cell to cell tranport	tumor necrosis; trimer, 52 kDa; hydrophilic	plasma, 6−16 pg/mL; sweat, 9−21 pg/mL; urine, 0.03−0.4 ng/mL	plasma, 0.1−0.3 pM; sweat, 0.2−0.4 pM; urine, 0.6−8 pM	immune cell regulation; immune response; disease fighting process

[a]References for biomarker concentrations: α-amylase;[29,44−47] BDNF;[48−52] cortisol;[43,53−58] CTT[59,60]; dopamine;[61−63] epinephrine;[64] IL-6;[65−67] norepinephrine;[68−71] NPY;[72−75] orexin A;[76−78] oxytocin;[79,80] serotonin;[81−84] TNF.[85]

DOI: 10.1021/acssensors.8b00726
ACS Sens. 2018, 3, 2025−2044

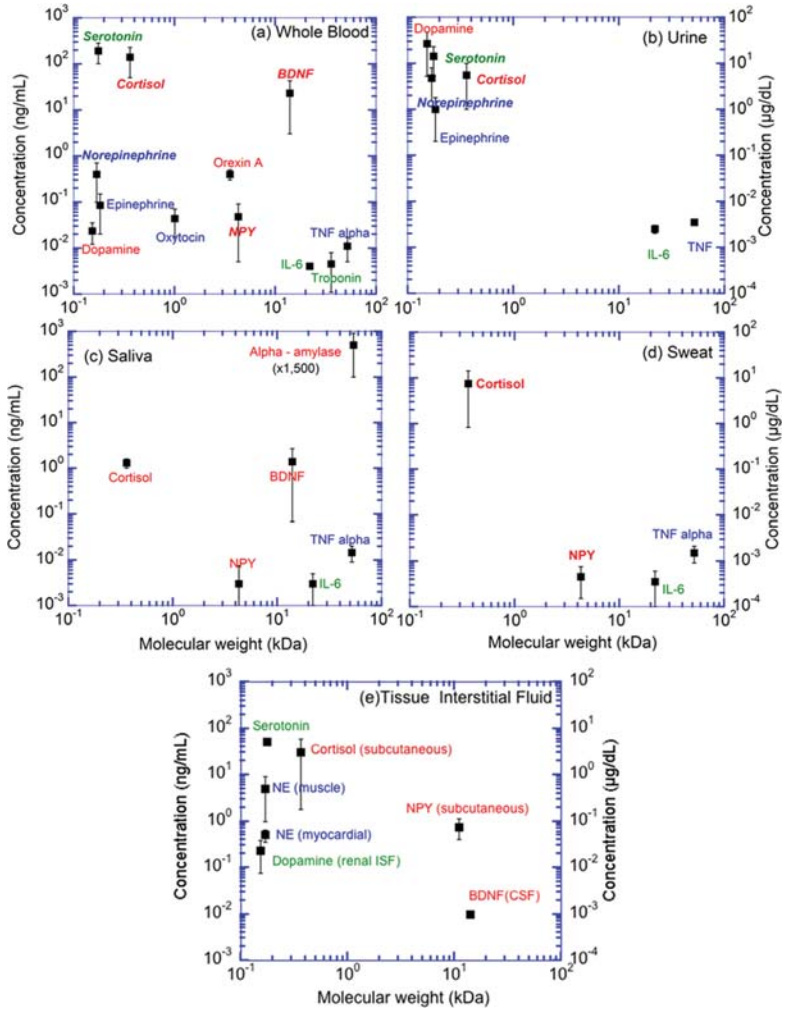

Figure 3. Biomarker concentration as a function of molecular weight in bodily fluids. Color code: red, lipophilic; blue, hydrophilic; green, amphiphilic.

render the molecule water-soluble, whereas nonpolar hydrocarbon chains yield hydrophobic properties.[33] Lipophilic biomarkers can become attached to lipids or proteins present in the solution,[34] with the bound molecule having different properties than the free analyte. Hydrophilic, amino acid biomarkers are considered to have surface-based interaction with protein molecules, through hydrogen bonding.[34]

Selected properties of 13 stress-related biomarkers obtained from an extensive literature survey are shown in Table 1. The list includes hormones (such as cortisol, troponin), neurotransmitters (such as dopamine, serotonin), and biomarkers that are generated by both the endocrine and nervous systems (such as epinephrine, norepinephrine). One enzyme biomarker (α-amylase) is also included for reasons discussed below. The biomarker properties summarized in Table 1 include the origin and transport mechanism in the body, molecular type and weight, physiological concentrations in relevant bodily fluids (e.g., blood, urine, sweat, saliva), and related health conditions that occur when the concentration is outside the normal range. The concentration format most frequently found in the literature is in units of weight per unit volume (such as ng/mL). For convenience, the calculated equivalent molar concentration is also listed for biomarkers consisting of small molecules. Key references regarding the concentration of each biomarker are also included in Table 1. The biomarker concentration can be obtained with a variety of sensing techniques, including colorimetric,[35] electrochemical,[36] immunochemical detection techniques,[37] mass spectrometry,[38] and nuclear magnetic resonance.

As can be seen in Table 1, a range of concentrations are reported for most biomarkers found in various bodily fluids. In a few cases, the concentration ranges reported are fairly narrow (ca. ±50%), but in many cases the reported range can vary by more than an order of magnitude. In select cases, the biomarker concentration is known to vary during the 24 h cycle, with cortisol and DHEA (dehydroepiandrosterone) being two such examples.[39,40] It is also likely that the biomarker type and concentration detected can be partially dependent on measurement technique, the condition of the instrumentation, and sample extraction and condition.[41,42] For example, the concentration of cortisol in sweat detected using ELISA is generally reported in the range of 8−142 ng/mL. However, measurements using HPLC-MS have reported a considerably lower concentration range.[43] The authors indicated that possible reasons for the lower concentration which they reported include the higher selectivity of their technique which differentiates between closely related hormones and metabolites with similar structures.

DOI: 10.1021/acssensors.8b00726
ACS Sens. 2018, 3, 2025−2044

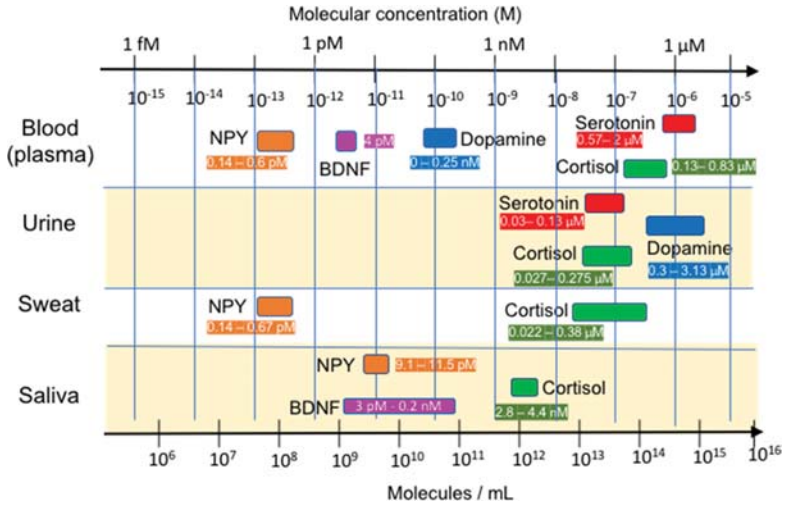

Figure 4. Molecular concentration ranges of key stress biomarkers in bodily fluids.

Table 2. Glossary for Materials and Components Used in Bioassays

biological and material terms	simple description
analyte	target molecule being identified and measured
aptamer	small single stranded oligonucleotide that folds into well-defined 3D structure and interacts with high affinity and specificity with target molecule
antibody	protective protein (generally of high molecular weight) produced by immune system in response to presence of antigen
antigen	foreign protein evoking an immune response (either alone or after conjugating with a larger protein molecule) and is capable of binding with a product (such as antibody or T cell) of the immune response
biomarker	biological molecule found in blood, body fluids, or tissues that may signal abnormal process, condition, or disease
carbon nanotube, CNT	hexagonal lattice of carbon rolled into cylinder with ∼100 nm and 1−2 nm sheet thickness; CNTs can be fabricated with single outer wall of carbon or multiple walls (cylinder inside other cylinders of carbon); CNTs possess extraordinary electrical conductivity, high tensile strength, high thermal conductivity
nanoparticle, NP; metal, Au; magnetic	ultrafine particle spanning 1−100 nm in diameter; physical and chemical properties of NPs depend on particle size and shape, and can vary from parent metal (e.g., magnetic NPs show superparamagnetic property which leads to higher magnetic susceptibility than traditional paramagnets); functionalized NPs have many uses in biomedical applications, e.g., imaging of cells and tissue, target molecule labeling, and drug delivery

While some more detailed information on most of the biomarkers in Table 1 is presented in the next sections of the review, key biomarkers that feature prominently in one or more bodily fluids are serotonin, cortisol, dopamine, BDNF, and NPY. The ranges of molar concentration and the equivalent number of molecules per milliliter of these 5 biomarkers in blood (plasma), urine, sweat, and saliva are shown in Figure 4. Cortisol is the only biomarker present in fairly large concentrations in all four bodily fluids. Serotonin and dopamine appear in significant quantities in blood and urine. BDNF is present in blood and saliva, at slightly smaller weight concentrations than cortisol. NPY and BDNF are polymers with larger molecular weights (as opposed to the small molecule nature of the other three biomarkers), which are found with low weight concentration and even lower molar concentration in most biofluids.

POINT-OF-USE SENSORS FOR STRESS BIOMARKERS

Traditional analytical methods for detecting and measuring biomarkers include X-ray diffraction (XRD), mass spectrometry (MS),[86] nuclear magnetic resonance (NMR), and liquid or gas chromatography (LC/GC).[87] These analytical methods (see brief descriptions in Table 3) can provide a wealth of information about the analytes present in the sample under test, such as structure, molecular weight, concentration, and identification, with high selectivity and precision over a wide dynamic range. However, the equipment associated with these methods represents a significant investment, requires operation by highly trained personnel, and frequently requires specialized laboratory space. In addition to the high cost aspect is the length of time required for full analysis.

There has been considerable growth in development/investigation of point of care/use diagnostic platform for stress and human performance measurement[88] in order to bring the biomarker measurement process closer to the individual and to reduce the cost. Point of care/use (PoC/PoU) diagnostics play an important role in guiding timely patient care in primary care settings.[89] PoU devices for biosensing applications designed to detect and quantify target molecules (such as proteins, nucleic acids, disease-specific antigens) are important tools of wide interest in medical diagnostics. Considerable progress has taken place in the development of sensitive and specific PoU detection systems,[90] with selective focus toward detection of biomarkers in biological fluids where detection specificity is a key factor. A glossary of commonly used terms in biosensing technology is given in Table 2.

Sensors to detect and measure the concentration of various biomarkers require transducers that convert energy from one form to another.[91] They are typically fabricated by immobilizing a biological receptor material on the surface of a

DOI: 10.1021/acssensors.8b00726
ACS Sens. 2018, 3, 2025−2044

Table 3. Brief Description of Key Detection Techniques[a]

detection techniques	simple description
colorimetric detection (PoC, benchtop, labeled)	technique of biomolecule (single of protein conjugated complex) detection based on color of target molecule complex, through spectroscopy or visual standards
electrochemical impedance spectroscopy (EIS) (laboratory, labeled, label-free)	highly sensitive spectroscopic technique to track changes and interactions at surfaces, impedimetric biosensing technique
electrochemical (EC) detection (benchtop, laboratory, labeled, label-free)	sensing of target analyte via electrochemical transduction; EC biosensor can provide specific quantitative or semiquantitative analytical information using biological recognition element (biochemical receptor) in direct spatial contact with EC transduction element. biological recognition system generates signal
electro-immunochemical (EIC) (benchtop laboratory, labeled, label-free)	immunoassay detection technique coupled with EC signal transduction for quantitative detection; subgroup of EC detection technique
ELISA (benchtop, labeled)	enzyme linked immunosorbent assay based on antigen−antibody−enzyme for detection and quantification of proteins, peptides, antibodies, and hormones
FTIR (laboratory, label-free)	Fourier transform infrared analysis provides information about bond structure of compounds, based on IR absorption of target molecule (vibrational and rotational characteristics of dipolar chemical compound); widely used for identification of target molecules
impedimetric detection (benchtop, laboratory, labeled)	impedimetric detection monitors change of dielectric properties and/or thickness of dielectric layer at electrode−electrolyte interface due to presence of target biomolecule interation with receptor immobilized at dielectric surface
label-free detection	based on detection of target biomolecule through recognition or identification of intrinsic physical property of molecule, e.g., optical, electrical, and acoustic
labeled detection	based on detection of tertiary complex formed by integration of primary biomolecule and secondary tag (such as fluorescence, NP, Ab-protein complex)
lateral flow immunassay (LFIA) (PoC, benchtop, labeled)	immunoassay, detect presence of target biomolecule based on capacity to act as antigen, exploiting unique binding ability with antibody; LFIA is paper-based immunoassay platform for detection and quantification of target biomolecule in complex mixture, where target sample is placed in test device and result are displayed within ∼5−10 min
mass spectrometry (MS) (laboratory, label-free)	detection and quantification technique based on individual molecular mass-to-charge ratio; apart from quantitation of target analyte in simple and complex mixture, mass spectrometry identifies individual molecule characteristics, e.g., structure, orientation, size, and composition; it is used in proteomics, drug discovery, and biomarker detection
nuclear magnetic resonance (NMR) (laboratory, label-free)	target analyte is exposed to magnetic field; nuclei absorb and re-emit EM radiation at particular resonance frequency, providing information about structural orientation of analyte at molecular and atomic level; provides physical, chemical, and electronic structural information on biomolecules in liquid or solid state; highly sensitive detection, particularly for compound identification, identification of active protein enzyme sites, and purity analysis
optical detection (PoC, benchtop, laboratory, labeled, label-free)	analysis of optical field and target biorecognition element; can be either labeled or label-free; in label-free mode, optical signal is generated directly by target analyte; labeled mode incorporates use of label (fluorescence, colorimetric, etc.) and optical signal generated by complex formed by target-molecule and label
surface plasmon (laboratory, labeled)	collective oscillation of free electrons in conducting media at defined wavelength and frequency, can be described as electron cloud coherently displaced from equilibrium position around lattice of positively charged ions in metallic surfaces, specific plasmon modes can be excited with external electric field; in metallic nanoparticles, with size comparable to skin depth, plasmon excitation is used for biomolecule sensing
ultraviolet and visible (UV−vis) spectroscopy (benchtop, laboratory, label-free)	measurement of attenuation of light upon its passage through (or after reflection) from target analyte; molecules absorb light within spectral range 190−900 nm (depending upon molecular weight, structure, composition); absorption wavelength is characteristic of molecule; prominent method for quantitative label-free detection of biomolecules
X-ray diffraction (XRD) (laboratory, label-free)	used for obtaining information about crystallographic structure and physical property of target molecule; target sample is irradiated with monochromatic X-ray beam over variable incident angle range; interaction results in diffracted X-rays when Bragg equation is satisfied, resulting spectra are characteristic of chemical composition and phase of molecule

[a]Colorimetric;[118] EIS;[119−121] electrochemical;[88,122] EIC;[37,123] ELISA;[124,125] FTIR;[126,127] impedimetric;[128,129] LFIA;[100,130] mass spectrometry;[43,131,132] NMR;[133,134] optical;[135] surface plasmon;[136−138] UV spectroscopy;[139] XRD.[140,141]

DOI: 10.1021/acssensors.8b00726
ACS Sens. 2018, 3, 2025−2044

suitable transducer that converts the generated biochemical signal into quantifiable electronic signals.[92] Historically, transducers referred to conversion between mechanical and electrical signals, such as that occurring in piezoelectric crystals.[93] However, over time, a broader definition has become accepted that includes other energy converting mechanisms. As schematically illustrated in Figure 5, the presence of biomarkers in biological fluids can be detected using a variety of transduction mechanisms.

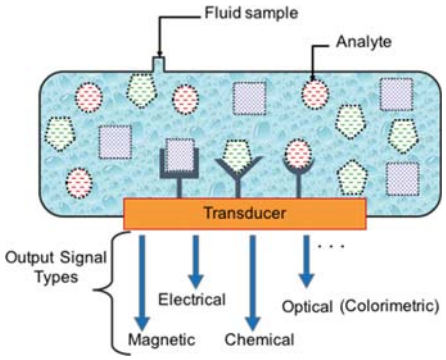

Figure 5. Biomarker sensor methods.

Target analytes are either directly detected or indirectly detected by their chemical interaction with biological receptor molecules (antibody, aptamer, DNA, RNA). A recent review of signal amplification and transduction approaches in PoC/PoU diagnostic systems using microfluidics technology was published by Jung et al.[94] Techniques for PoC/PoU detection of biomarkers specifically in bodily fluids have been reported using immunoassay,[95] surface plasmon resonance,[96] electrochemical reaction,[97] fluorescence,[98] and chemiluminescence.[99]

Prominent material platforms used in fabricating PoU biosensor devices are primarily paper (cellulose, nitrocellulose), glass, and flexible polymers. The latter includes polydimethylsiloxane (PDMS), poly(methyl methacrylate) (PMMA), and cyclic olefin polymer (COP) and copolymer (COC). Less frequently silicon platforms are also reported. Substrate selection is a function of many factors, including detection mechanism, biocompatibility, sensitivity, multiplexing ability, device reusability, and cost.

Paper-based platforms are usually lateral flow assay (LFA)-based, either immunoassays or chemical colorimetric assays. Lateral flow immunoassays (LFIA) consist of prefabricated strips of a carrier material, different parts of which are assembled on a plastic backing. These components typically are sample application pad, conjugate and/or blocking pad, nitrocellulose (NC) transport membrane and absorption ("wick") pad. The NC membrane contains immobilized reagents that interact with the analyte solution and form the test and control lines for the assay.[100] The sample application pad is made of cellulose or glass fibers. The liquid sample is dispensed onto the pad to start the assay. The conjugate pad typically contains labeled immobilized biorecognition molecules that are released upon contact with the input liquid. A schematic of a typical LFA strip is shown in Figure 8a.

The NC analytical membrane is the most critical part of the assay and it determines the sensitivity of the assay. Properties of the NC membrane that affect assay reproducibility and sensitivity[101] include sample flow rate, porosity, wicking rate, nonspecific adsorption on test and control lines. The adsorbent pad functions as a sink at the end of the strip.[101] Important features of LFA-based biomarker sensing[102] include assay rapidity, one step analysis, low operational cost, simple instrumentation, user-friendly format, little or no interference due to chromatographic separation, high specificity, good sensitivity, long-term stability under different set of environmental conditions, and portability. Most importantly, since the sample flows in the device due to the capillary force, no external fluidic controls are needed. Therefore, a small package and a low cost can be obtained. Some of the challenges of this approach include sample liquid evaporation, vulnerability to environmental condition such as humidity, protein (present in target sample) incompatibility with surfactants that impacts its binding ability with the membrane, and occasional inconsistency in flow characteristics due to desiccation,[103] which sometimes can compromise assay sensitivity.[104]

Polymeric materials have been identified as attractive substrates for PoU devices owing to their mechanical flexibility, light weight, mass fabrication capacity, low cost, and availability in different grades with multiple varying physical/chemical properties as per device/functionality requirement,[105] including optical transparency, heat conductivity, electrochemical resistance, and biofluid compatibility.[106] Polymers, such as PDMS, PMMA, polypropylene, and hydrogels, have high optical transmissivity in both UV and visible range. Hence, they can be used in various optical detection platforms, for example, photonic nanosensing[107] and SPR.[108] PET (polyethylene terephthalate) is a polymer with high heat conductivity and stability at very high temperature (melting point of 260 °C), which would be suitable for temperature controlled biological reactions.[109] COC and COP polymers are electrochemically inert and have high optical transparency, and hence, they can be used in electrochemical immunosensing approaches with optical detection transduction.[104] Polymers can also be engineered into thin, flexible, bendable substrates with self-healing capability[110] that can be used for implantable and wearable devices.[111] Unlike capillary flow in the paper-based platform, polymer-based devices require pump-controlled flow, which can deliver liquid with great precision, but in a more complex overall system and at a much higher price point.

Silicon based MEMs biosensors have also been reported for PoU biosensor applications,[112] either in nanowire form[113] or in the form of primary substrate.[114] Biosensor devices fabricated on silicon wafers have application limited to in vitro biosensing, owing to their in vivo incompatibility. Hence, Si based integrated circuits require biocompatible packaging in order to be used within living tissue. Interestingly, nanostructured porous Si based biosensors have gained popularity in recent years[115] owing to their attractive features, such as ease of fabrication, tailored morphological structure, versatile surface chemistry,[116] and higher biocompatibility than Si.[117]

In this review, the reported techniques for PoU detection of stress and key human biomarkers in different body fluids are reviewed. Biomarker detection can either use a separate "label" for detection or be "label-free", as illustrated schematically in Figure 6. Labeled detection is generally implemented by use of functionalized nanoparticles, performing various functions. A common example is the use of Au nanoparticles for optical detection in the form of a color change in the presence of a specific biomarker.[35] Another example is the use of functionalized

DOI: 10.1021/acssensors.8b00726
ACS Sens. 2018, 3, 2025−2044

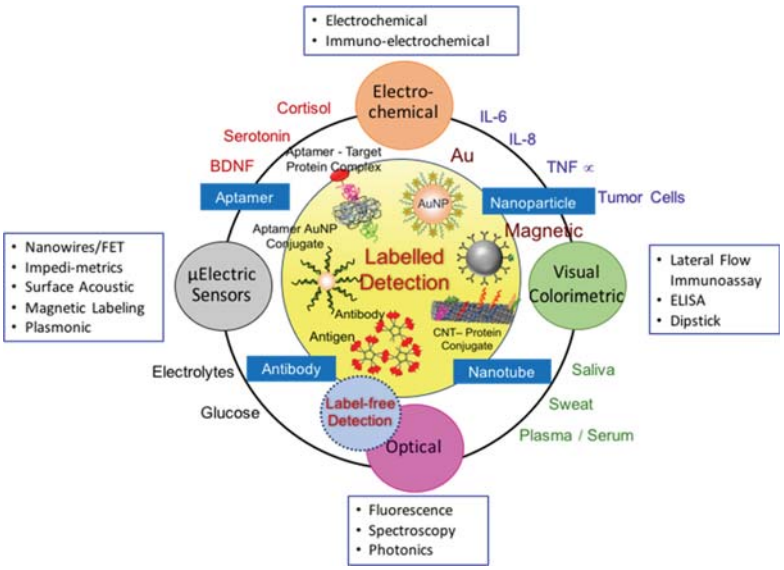

Figure 6. Mechanisms and materials for point-of-use biomarker sensors.

magnetic nanoparticles. When these particles are conjugated with an antibody complex specific to the target biomarker an external magnetic field can be used to separate out the antigen−antibody magnetic nanoparticle complex.[142,143] Label-free detection techniques include optical spectroscopy.

A comprehensive literature survey was conducted regarding the various methods used for the PoU/PoC detection of 6 stress-related biomarkers (cortisol, troponin, dopamine, NPY, IL-6 and BDNF) in bodily fluids and/or buffer solution. The detailed results of the survey are contained in Tables 4−6, including the biofluid medium, the detection method, and the limit of detection.

A listing of materials, components and fabrication equipment utilized in each case has been included in an extended version of Tables 4−6 in the Supporting Information. Using information from the Supporting Information table allows for a comparison of various approaches for suitability in specific applications. An example of this comparative analysis is shown in Table 7 for the detection of cortisol. It is hoped that similar analyses for other biomarkers would be useful for the readers of this review.

The detection process starts with obtaining a sample of the desired bodily fluid (e.g., blood, urine, saliva), which is then introduced into or onto a "detection" device. In the so-called "dipstick" approach, the device is simply a small vial containing the recognition molecules for the analyte of interest along with the label molecules. Many commercial and experimental PoU test devices use the lateral flow assay (LFA) platform where the liquid sample under test is dispensed onto a device consisting of a stack of porous membranes.[130] This allows for the fluid sample to flow without the need of external pumps or other accessories.[100] The label and recognition molecules are contained in various regions of the LFA stack and upon hydration by the sample interact with the relevant biomarker as it flows through the device.[145,154] Biorecognition molecules are immobilized in two stripes, the "test" and "control" lines, downstream from the sample dispensing location, where they can interact with the target analyte.

A variety of approaches have been developed for the detection of biological analytes in LFAs.[182,183] Some of the main approaches are illustrated in Figure 7. The biorecognition molecule can be an antibody (in which case the platform is known as an immunoassay, LFIA), an aptamer (short sequences of single stranded nucleic acids), or an enzyme. The selection of the biorecognition element is based on its ability to bind to the target analyte with high affinity and selectivity. The simplest approach (Figure 7a) uses direct detection of the analyte captured by the biorecognition molecules immobilized in the test and control lines. Reporter (or label) molecules are introduced that will bind to the analyte and generate a measurable (usually optical) signal. For many analytes, the signal and specificity produced in the direct detection method is too low. Improvements in LOD and specificity are obtained using the "sandwich" detection approach (Figure 7b), where a second biorecognition molecule (efficiently conjugated to a detection label) is introduced to form a sandwich structure with the analyte held in between. In the competitive detection scheme (Figure 7c) a known amount of preconjugated analyte is introduced together with the unknown amount of target analyte, with both competing for the fixed number of binding sites of the biorecognition molecules immobilized on the surface. In this case increases in the target analyte concentration result in a decreasing detected signal.

Colorimetric detection is widely utilized in well-established commercial technology PoC diagnostic devices, such as the urine test strip (Figure 8b) where a single strip simultaneously detects multiple biomarkers in urine, and pregnancy tests strips (Figure 8c). The basic format of colorimetric LFA biosensors utilizes a nitrocellulose membrane strip onto which test and control lines are formed by preimmobilizing specific reagents. Upon activation during contact with the target sample, a change of color or visibility of the test or control line (or both) occurs depending upon the designed chemistry. This is the indicator of the presence of target biomolecules in the sample.[184] As shown in the example of Figure 8d,[95] detection of the cardiac stress biomarker troponin 1 is reported using AuNPs of different sizes (10 nm, 40 nm). It is observed that increasing troponin 1 concentration leads to higher visibility test line. Improved results are obtained with simultaneous use of both 10 and 40 nm AuNPs, yielding a reported LOD of 10 ng/mL. Colorimetric detection can also be implemented

DOI: 10.1021/acssensors.8b00726
ACS Sens. 2018, 3, 2025−2044

Table 4. Selected Published Highlights of Cortisol and Troponin Biosensors

biofluid	LOD, range	detection mechanism	ref
		cortisol	
saliva	1 pM to 10 nM	immuno-EC impedance	144
saliva	0.3−60 ng/mL	immunoassay-coupled with chemiluminescence	145
saliva serum	∼10 pg/mL	aptamer-AuNP based EC detection	146
serum	10−80 μM	Au nanowire-based EC detection coupled with immunoassay	147
plasma, saliva, urine	pg/mL range	EC luminescence immunoassay, immunochemiluminescent assay	148
saliva	0.36 ng/mL	SPR coupled with immunoassay	149
saliva	0.1−10 ng/mL	EC immunoassay with fluid control design for on-chip pretreatment of sample	150
sweat, saliva	0.1 ng/mL (cortisol) 0.1 mM lactate	electrochemical chronoamperometric detection	151
sweat	1 pg/mL (synthetic sweat); 1 ng/mL (human sweat; range 10−200 ng/mL)	electric double layer modulated biosensing	152
		troponin	
buffer	1−100 ng/mL	EC detection of antitroponin and troponin interaction on conducting paper using aniline polymerization on screen-printed paper electrode	153
plasma	0.03−6.5 ng/mL (linear range)	optomagnetic biosensor−sandwich immunoassay performed on stationary liquid assay	154
serum	0.01−5 ng/mL (PBS); 0.07−6.9 ng/mL (human serum)	capacitive biosensor coupled with immunoassay	155
buffer	0.092−46 ng/mL	SiNW based FET sensor responsive toward interaction between immobilized troponin antibody and protein	156
plasma	0.1 ng/mL	photonic crystal total internal reflection (PC-TIR)	157

Table 5. Selected Publication Highlights of Dopamine Biosensors

biofluid	LOD, range	detection mechanism	ref
		dopamine	
buffer (PBS)	0.085−700 ng/mL	SPR using D3 dopamine receptor as recognition element (SPR coupled with immunoassay)	158
buffer	2.5 μM	colorimetric detection, plasmon absorbance of Au-NP mediated by exposure of dopamine, adrenaline, NE	159
buffer in vivo (corpus striatum of rat)	1−5 μM (dopamine and serotonin)	electrochemical detection of CNT coated carbon fiber microelectrode for simultaneous detection of dopamine and serotonin	160
in vivo (rats)	physiological range (sensor responds to dopamine release)	voltammetry microsensor	161
buffer	10 μM	SPR sensor chip (Au−film: molecular imprinted polymer gel; AuNP immobilized polymer gel)	162
buffer	33 nM to 3.33 mM	colorimetric detection, AuNP−dopamine interaction in presence of melamine	163
buffer	20 pM; range 0.1−10 000 nM	fluorescence intensity (ds-DNA and CuNP) quenching with increasing DA concentration	164
buffer	50 nM for DA; 250 nM for 5-HT	dynamic pulse voltametric sensing	165
buffer	0.5 μM (linear range: 10 μM to 1 mM)	self-powered triboelectric nanosensing	166
serum	0.04 μM (linear range: 0.5−100 μM)	electrochemical detection	167
buffer, cell culture media, simulated body fluids	10^{-10} M	SERS	168
serum CSF	20 nM	colorimetric detection using modified AuNP	169

in solution phase with AuNPs as the primary agent,[185] as shown in Figure 8e where AuNPs aggregate and change color linearly upon exposure to the biomarker dopamine, serotonin, and adrenaline.[159] Change in color can be quantified with absorption spectroscopy to evaluate the biomarker concentration.

Other detection approaches aim to provide an indication of the presence and concentration of specific biomarkers without the need for an optical label. For example, ion sensitive (IS) field effect transistors (FET)[186] take advantage of changes in current that result when ions in solution come in contact with an ion-selective membrane in the gate region of the FET.[187] ISFET biosensors utilize recognition molecules immobilized on the gate insulator to capture specific biomolecules from the analyte solution.[188] In turn, the charges associated with the biomolecules modify the current flow in the ISFET.[189]

Selected examples of the prominent detection techniques reported for stress biomarker detection in point of use platform are discussed in the following sections.

Immunoassay. Immunoassay detection technique is based on interaction of a target analyte (protein, nucleic acid, and antigen) with its corresponding antibody. The antigen−antibody complex formation is a measure of the concentration of the antigen present in target sample. Typically, the antibody is labeled with nanoparticles (Au, magnetic, fluorescence, and chemiluminescent enzyme) to provide a detection signal. Transduction in immunoassays can be visual/colorimetric, fluorescence based, and chemiluminescence based.

Visual/Colorimetric. A common approach implemented through immunoassay is colorimetric detection wherein a color change is detected and the intensity of the color is an indication of the concentration of the biomarker molecule.[190] This approach uses a reporting probe or "label" (such as Au nanoparticles, AuNPs) attached to a recognition molecule (such as antibodies or DNA/RNA aptamers)[118] that will selectively bind with the molecule of interest in order to indicate its presence and evaluate its concentration in the sample under test.[191]

DOI: 10.1021/acssensors.8b00726
ACS Sens. 2018, 3, 2025−2044

Table 6. Selected Publication Highlights of NPY, IL-6, and BDNF Biosensors

biofluid	LOD, range	detection mechanism	ref
		NPY	
buffer saliva	10 pM range	ELISA (AuNP enhanced)	178
buffer	pM level from sub-nL sample	EC detection coupled with electro kinetic sample preconcentration	179
buffer	10 pM	aptamer functionalized NPY detection	180
		IL-6	
serum, synovial fluid	1 pg/mL	ELISA	170
serum (calf)	0.5 pg/mL	EC immune-sensing (CNT based)	97
serum (human)	IL-6, IL-8, 5-15 fg/mL	EC immunosensing detection	171
buffer	4.7 pg/mL	graphene oxide-based amperometric field effect transistor (FET) sensing	172
buffer	0.38 pg/mL (range 1 pg/mL−100 ng/mL)	photoelectrochemical immunoassay	173
		BDNF	
buffer CSF	pg/mL	impedance measurement, interaction of BDNF and BDNF antibody immobilized on electrode surface.	174
serum	5−7 ng/mL	SPR sensor chip	175
plasma	0.1−2 ng/mL	electrochemical, immunosensing	176
serum	5 pg/mL (linear range 0.01−100 ng/mL)	electrochemical, immunosensing	177

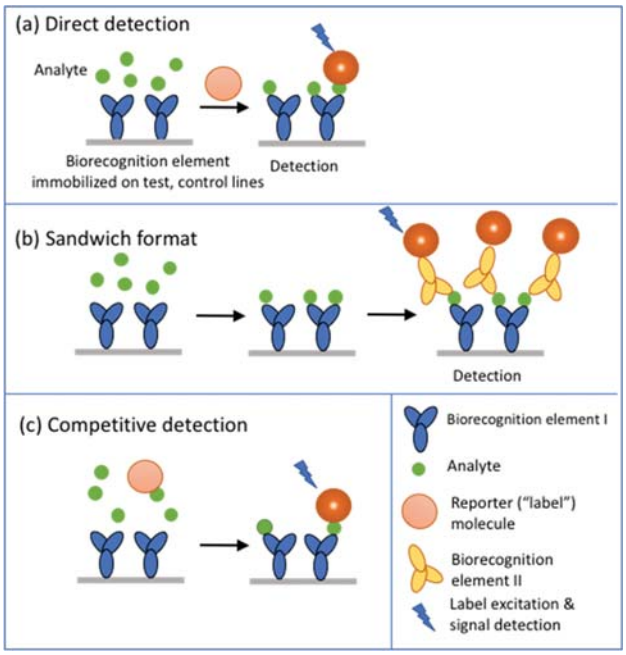

Figure 7. Detection approaches for point-of-use lateral flow assays. Adapted with permission from ref 182. Copyright 2008 American Chemical Society.

Colorimetric immunoassay is usually implemented in solution phase or on paper (lateral flow, chromatographic paper). The detection strategy of colorimetric immunoassay is based upon biochemistry of the assay design, such that there is an element of color change when contact occurs with the target analyte.

AuNPs are a common label used in colorimetric assays because of their high sensitivity and superior capability of visual detection with the naked eye.[192] Gold nanoparticles have high affinity toward biomolecules. The optical properties of AuNPs are dependent on shape (spherical[193] or anisotropic[194]) and size, and on ability to aggregate and change color upon interaction with analytes in target samples.[101,195] Solutions containing AuNP colloidal suspensions normally appear reddish in color due to coherent oscillations (so-called surface plasmons) of surface electrons induced by the electromagnetic field of incident visible light.[196] For example, AuNPs with 13 nm diameter exhibit peak absorption at a wavelength of ∼520 nm and appear red to the eye.[197] The absorption plasmon spectral band varies slightly with AuNP size. With increase in size of the AuNPs, the surface plasmon band becomes broader and a red shift is observed due to non-homogenous polarization of surface electrons.[197] Upon interaction of the AuNPs with the target analyte molecules, the NPs aggregate into a cluster (which can be considered as a single large particle), resulting in a change in color of the solution from red to blue. The level of aggregation and resulting change in color intensity are dependent upon the analyte concentration.

Fluorescence. Use of fluorescent labels (such as dyes, proteins) in immunoassay has become more prominent over the past decade primarily because of higher assay sensitivity and quantitative measurement. In fluorescence-based assays, the capture mechanism remains the same, wherein the target analyte interacts with an antibody or aptamer labeled with fluorescent dye. The fluorescence signal is measured in a separate reader system, where excitation of the fluorescent molecules is externally provided and the emitted light (proportional to the target analyte concentration) is measured.[198] In addition to fluorophores consisting of organic molecules, inorganic quantum dots are used in bioassays owing to their high emission brightness level, size-tunable fluorescence emission, narrow spectral line widths, large absorption coefficients, and excellent stability against photobleaching.[102]

Chemiluminescence. Chemiluminescence (CL) can occur during certain chemical reactions where relaxation of molecules

Table 7. Comparative Analysis for the Detection of Cortisol Using Methods Reported in the Literature[a]

biomarker	label, detection method	preparation complexity	key component no.	instrumentation and material cost	LOD	ref
cortisol	Ab-EIS	medium	6	medium	ng/mL	181
	Ab-chemiluminescence enzyme	medium	7	medium	ng/mL	145
	aptamer-AuNP-EC	high	14	high	pg/mL	146
	AuNW-Ab-EC	high	12	high	ng/mL	147
	Ab-ECLIA	medium	5	medium	pg/mL	148
	Ab-SPR	medium	7	medium	ng/mL	149
	Ab-EC	medium	11	medium	ng/mL	150

[a]A comprehensive list for other stress biomarkers is found in Tables 4−6 and in the Supplementary Information.

DOI: 10.1021/acssensors.8b00726
ACS Sens. 2018, 3, 2025−2044

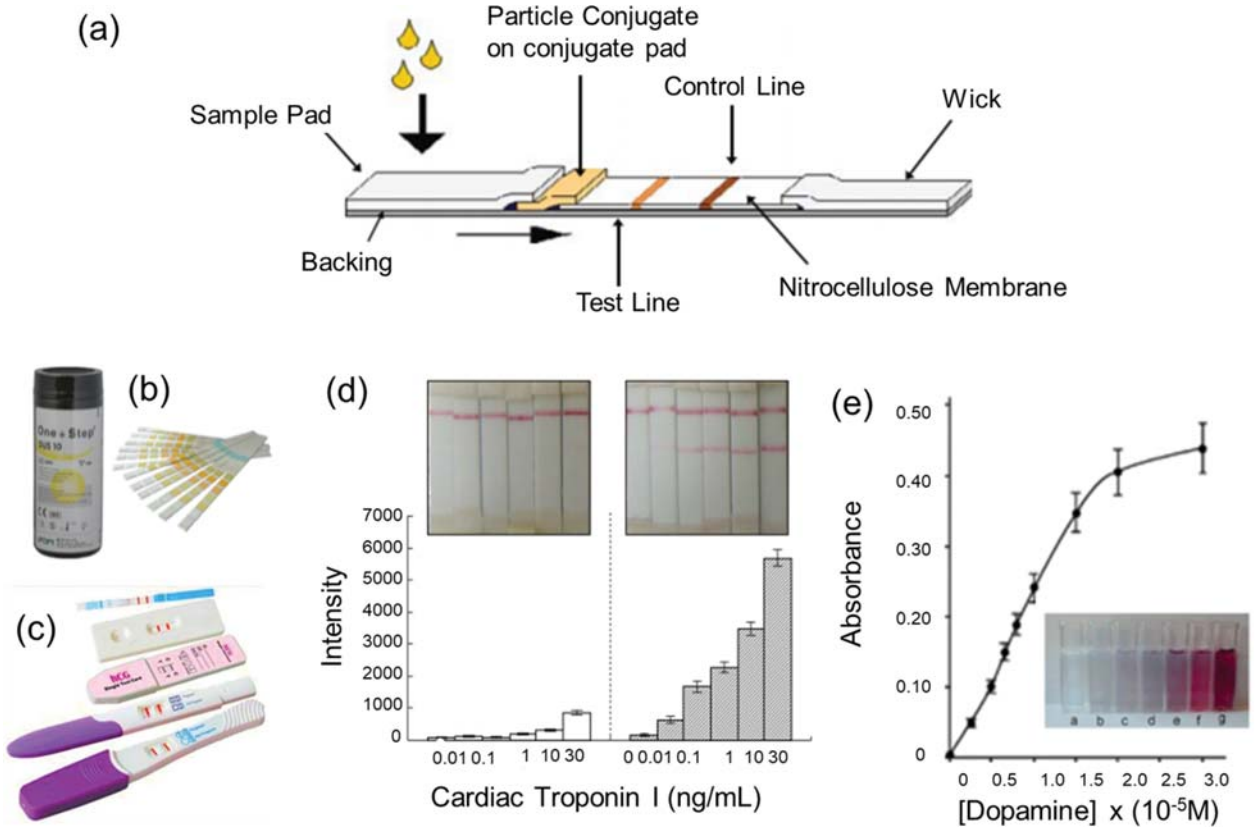

Figure 8. LFA based detection of biomarkers: (a) standard configuration of lateral flow immunoassay strip. Reprinted with permission from O'Farrell, B. Evolution in lateral flow based immunoassay systems. *Lateral flow immunoassay*, Springer: **2009**; pp 1−33.[130] Copyright 2009 Springer. (b) commercial urine test strips; (c) pregnancy test strips; (d) colorimetric detection of troponin 1 by LFA with AuNP size of 10 nm (left) and combined sizes 10, 40 nm (right). Reprinted with permission from Choi, D. H.; Lee, S. K.; Oh, Y. K.; Bae, B. W.; Lee, S. D.; Kim, S.; Shin, Y.-B.; Kim, M.-G. A dual gold nanoparticle conjugate-based lateral flow assay (LFA) method for the analysis of troponin I. *Biosens. Bioelectron.* **2010**, 25, 1999−2002.[95] Copyright 2010 Elsevier. (e) Detection of dopamine in solution using AuNP aggregation. Reprinted with permission from ref 159. Copyright 2005 American Chemical Society.

occurs by emission of light rather than transfer of thermal energy.[199] Chemiluminescence can be the product of certain reactions involving the mixing of reagents (oxidants and catalysts, such as enzymes), whereas bioluminescence involves living organisms and enzymes (luciferases). A CL reaction widely used in forensic investigations involves the use of luminol (small organic molecule) that produces a light emitting fingerprint of very minute traces of blood, catalyzed by iron in blood hemoglobin. CL has received considerable attention for biomarker assays by virtue of its simplicity, low detection limit, wide calibration range, and inexpensive instrumentation.[200] The principle of the immunoassay technique remains the same, only the detection is enhanced by enzymatic CL reaction. As an example, salivary cortisol detection using CL-LFIA has been reported.[145] This is a competitive immunoassay, where cortisol (in saliva) and horseradish peroxidase (HRP)-cortisol conjugate compete for anticortisol antibody. The visual signal is generated by enzymatic activity of the CL substrate with HRP−cortisol bound to antibody. The test line signal intensity is inversely proportional to cortisol concentration in saliva, with a reported LOD of ∼0.3 ng/mL. Chemiluminescence platform is dependent upon high efficiency optoelectronic components that would facilitate maximum collection of generated light or luminescence, such as photodiodes, photomultiplier tubes, CMOS, and thin film photosensors.[201]

Electrochemical Detection. Electrochemical detection of biomarkers offers robust quantitative measurement using relatively simple and low-cost instrumentation.[202] The EC technique is very sensitive and capable of detecting analytes in the femtomolar range. An electrochemical detection setup generally contains several electrodes (working, reference, and counter electrodes) and a solution containing the electrochemically active species. Upon application of potential, changes in the redox status of the target analyte can be detected and quantified. Various forms of EC detection (current flow at fixed or varying potential, AC and/or DC) are widely utilized. EC effects have been used as transducers for immunoassays. Figure 9 schematically illustrates a typical example of EC: immunoassay for detection of cortisol in saliva.[203] Here, zinc oxide in the form of nanoflakes or nanorods is used as the working electrode and platinum as reference electrode. Anticortisol antibodies immobilized on the working electrode surface bind with cortisol in saliva samples via electrostatic interaction, with the immobilized antibody quantified through cyclic voltammetry.[203] In this case, the LOD for cortisol is reported to be in the range of 1 pM.

In general, electrochemical detection offers very high sensitivity and has been extensively implemented for detection of stress biomarkers in body fluids. Arya et al.[144] report cortisol detection in saliva (range 1 pM to 10 nM) by using EC impedance spectroscopy, tracking the interaction between cortisol in

DOI: 10.1021/acssensors.8b00726
ACS Sens. 2018, 3, 2025−2044

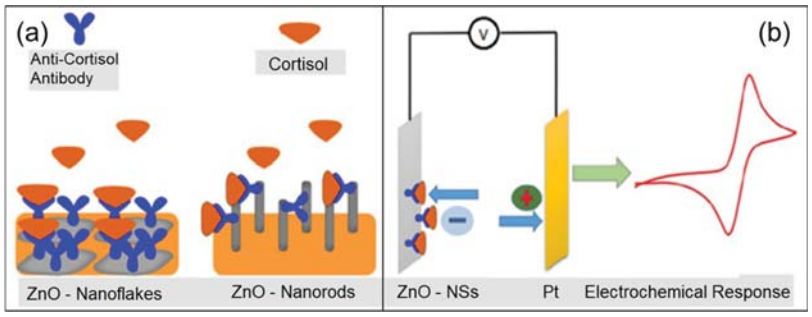

Figure 9. Cortisol detection using immunoassay and electrochemical sensing: (a) immobilization of anticortisol antibodies onto ZnO nanoflakes and nanorods; (b) illustration of EC response in the presence of cortisol. Reprinted with permission from Vabbina, P. K.; Kaushik, A.; Pokhrel, N.; Bhansali, S.; Pala, N. Electrochemical cortisol immunosensors based on sonochemically synthesized zinc oxide 1D nanorods and 2D nanoflakes. *Biosens. Bioelectron.* **2015**, 63, 124−130.[203] Copyright 2015 Elsevier.

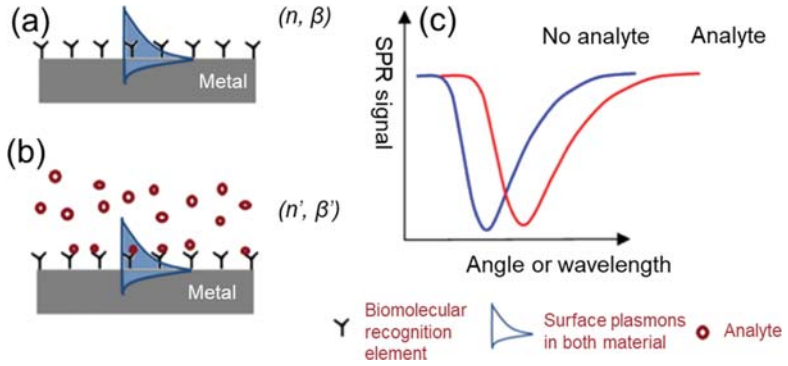

Figure 10. SPR biosensing principle: (a) surface plasmon propagation along metal surface; (b) recognition and capture of analyte molecules present in the liquid sample, producing a local change in the refractive index of the metal surface; (c) the refractive index change induces an SPR signal due to a shift in resonant angle or wavelength. Reprinted with permission from Guo, X. Surface plasmon resonance based biosensor technique: a review. *J. Biophotonics* **2012**, 5, 483−501.[96] Copyright 2012 Wiley.

target sample and antibody immobilized in the bioelectrode surface. Highly sensitive cortisol detection biosensor for both saliva and serum is reported[146] using aptamer-AuNP complex as the labeling agent immobilized on graphene coated carbon electrode surface. LOD for this work is 10 pg/mL, which is excellent. Jagadeesan et al.[153] report detection of cardiac stress biomarker troponin. The EC detection is performed on conducting paper substrate. Dopamine is an electrochemically active biomarker,[160] and hence, it can be detected directly without using immunoassay conjugation. Clark et al.[161] report a voltammetry microsensor using single carbon fibers encapsulated within fused silica as working electrodes for in vivo detection of dopamine in mice and rats.

Surface Plasmon Resonance. Surface plasmon resonance is an optical, label-free biosensing method, where detection depends on refractive index changes upon binding between target analyte (protein, nucleic acid, antigen) and corresponding capture molecules immobilized at the measurement site. Surface plasmons (SPs) are coherent electronic oscillations existing at the interface between two materials, changing dielectric function at the metal−dielectric surface. These evanescent waves propagate along the interface between a dielectric and a metal, with a decay length on the order of the oscillation wavelength.[204] Surface plasmons are very sensitive to changes in the boundary conditions, resulting in a high-resolution sensing method for biomarker detection in an external medium. Figure 10 illustrates the basic principle of an SPR biosensor.[96] The biomolecular recognition element is immobilized on the metal surface, where it can capture the target analyte producing a local increase in refractive index. In turn, this alters the propagation constant of surface plasmons, which can be measured using various optical methods (such as intensity modulation, wavelength modulation). The excitation of SPs at the metal−dielectric interface results in the transfer of energy from incident photons to SPs. The optical reflection intensity measured as a function of incident angle or wavelength reveals a sharp dip at the resonance angle or wavelength, which is strongly affected by the presence of captured analyte molecules. For sensor applications, the refractive index change of a thin layer in contact with the metal surface of the sensor is monitored by measuring the spectral shift of the resonance dip.[96,182] Common biorecognition elements used are antibodies, RNA aptamers, AuNPs, and magnetic nanoparticles. Sensitivity and selectivity of the SPR detection process highly depend on proper immobilization of biorecognition molecule on the SPR chip.[205]

In recent years, SPR based biosensing has been widely used for detection of stress biomarkers in different body fluids. Stevens et al. report[149] a portable SPR-based biosensor system fabricated on a Au surface combined with competitive immunoassay for quantitative detection of cortisol in saliva, illustrated in Figure 11. A gold surface SPR sensor chip was coated with cortisol-conjugated BSA (or plain BSA for the reference channel), followed by introduction of monoclonal anticortisol antibody. Upon introduction of varying concentration of cortisol in target body fluid (saliva in this case), change in refractive index slopes due to antibody binding with the

DOI: 10.1021/acssensors.8b00726
ACS Sens. 2018, 3, 2025−2044

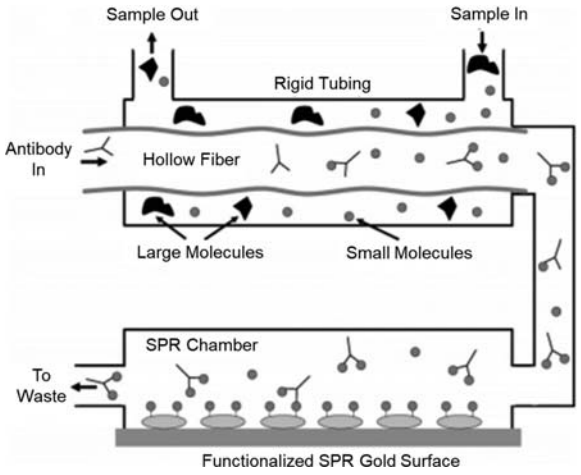

Figure 11. SPR system example: External, in-line filtering flow cell, which directs flow into the SPR system. Salivary samples were diluted 1:2 with buffer and flowed through tubing external to the hollow fiber. The antibody solution was flowed countercurrent through the hydrophilic hollow fiber and then through the SPR biosensor system. Reprinted with permission from ref 149. Copyright 2008 American Chemical Society.

cortisol-conjugated BSA surface was used to measure cortisol. The cortisol LOD reported is ~1 ng/mL.

The detection of dopamine has been reported[158] using the SPR sensing approach. D3-dopamine receptor has been used as recognition molecule of dopamine. Au-coated glass substrates were used as SPR sensor chips, where dopamine-BSA conjugate (DA-BSA) was homogeneously immobilized through physical adsorption. The indirect competitive interaction of dopamine receptor and DA-BSA with target dopamine was studied by SPR, with a linear detection range reported to be between 0.085 and 700 ng/mL. This simple assay procedure has potential to be incorporated for measurement of dopamine in actual biofluids. Plasmonic interaction of AuNPs is another SPR-based technique for detection of biomarkers.[206] The exposure of AuNPs in certain liquid environments results in their aggregation and a corresponding colorimetric signal. The absorbance of aggregated AuNPs upon exposure to certain biomarkers can be used as a method for quantification of biomarkers.[159]

SUMMARY, CHALLENGES, AND FUTURE PROSPECTS

In this review, we have discussed some of the basic properties of primary stress biomarkers (hormones and neurotransmitters), including their molecular structure, weight, and hydrophilic or lipophilic nature. Most importantly, their concentrations in various bodily fluids (blood, urine, saliva, and sweat) were summarized. The ultimate goal is to use this information for the design of improved PoC/PoU sensors that are able to detect relevant concentrations of the biomarkers in a low cost, easy to use package.

Current sensor options for biomarker detection were briefly reviewed. In reviewing the properties of biomarkers and sensor options, several challenges are apparent. Different biomarkers can have very different concentrations in any one fluid (by as much as 5 orders of magnitude), and the concentration of a given biomarker is likely to change significantly from fluid to fluid. For example, serotonin is found in relatively high concentrations (~100 ng/mL) in blood, urine, and tissue interstitial fluid, while it is effectively absent (<1pg/mL) in saliva

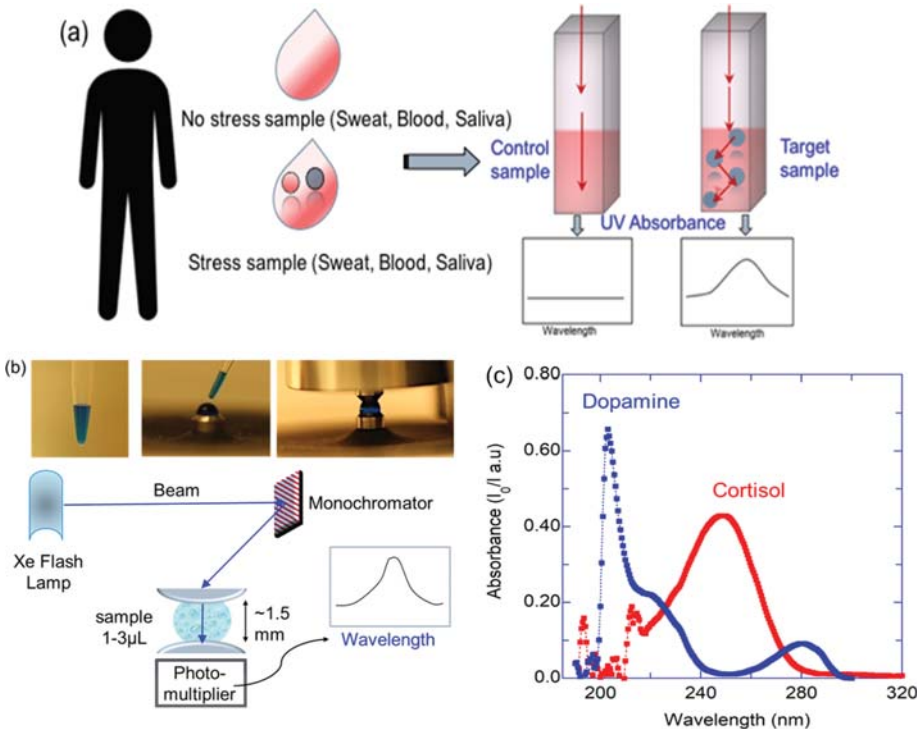

Figure 12. Optical absorption approach for label-free biomarker detection: (a) basic concept; (b) measurement setup: (c) UV absorption spectra of cortisol and dopamine in buffer solution indicating the separation between absorption peaks and related ability to distinguish between these two biomarkers.

DOI: 10.1021/acssensors.8b00726
ACS Sens. 2018, 3, 2025−2044

and sweat. Cortisol is found in similarly high concentrations in blood and urine. Interestingly, cortisol is also found in roughly the same concentration in sweat, whereas serotonin is absent. Cortisol is found in saliva at a concentration 100× lower than in the other bodily fluids (~1 ng/mL). In saliva, the detection of α-amylase with a significantly higher concentration (~1 mg/mL) is an option for stress level evaluation.

It is clear that high sensitivity is needed for accurate biomarker detection. It is likely that no one single sensor concept will work for the detection of all biomarkers. However, it may be possible to define subsets that can be served by one main biomarker type (e.g., small molecules vs polymers or hormones vs enzyme). Looking forward, another potentially important new direction is the simultaneous detection of multiple biomarkers that would combine to provide greater insight into the status of the individual being tested. A new approach that we are investigating is based on the optical absorption of stress biomarkers at near-UV wavelengths in order to develop simple point-of-use measurement systems that do not require the use of labels, recognition molecules, and complex measurement techniques and equipment. The principal idea behind the label-free optical detection approach (illustrated in Figure 12) is harnessing the absorption properties of each biomarker, which present unique UV absorption profiles tied to their molecular structure. Optical measurements can be performed with miniature stand-alone spectrometers, such as the NanoDrop One UV−vis spectrophotometer (Nanodrop Inc., Thermo Fisher Scientific), as shown in Figure 12b. An example is shown in Figure 12c that illustrates the ability to distinguish between the absorption of dopamine (with a peak at ~204 nm) and cortisol (at ~247 nm) in buffer soutions. This biomarker sensor approach can be extended to their detection in various biofluids (sweat, plasma, urine, and saliva). For eventual PoC/PoU implementation, we envision low cost optoelectronic integration with a LED light source and photodiode signal detection.

■ ASSOCIATED CONTENT

Supporting Information

The Supporting Information is available free of charge on the ACS Publications website at DOI: 10.1021/acssensors.8b00726.

Expanded table for Tables 4−6 summarizing publication highlights of cortisol, troponin, dopamine, NPY, BDNF, and IL-6 biosensor with list of materials, biosensor substrate, components, and equipment utilized (PDF)

■ AUTHOR INFORMATION

Corresponding Author

*E-mail: a.steckl@uc.edu.

ORCID

Andrew J. Steckl: 0000-0002-1868-4442

Prajokta Ray: 0000-0001-6262-9021

Notes

The authors declare no competing financial interest.

■ ACKNOWLEDGMENTS

This work was supported by the National Science Foundation and by the industrial members of the Center for Advanced Design and Manufacturing of Integrated Microfluidics (NSF I/UCRC IIP-1738617) and by UES Inc. (S-104-000-001) as a subcontract from AFRL (FA8650-15-C-6631).

■ VOCABULARY

biomarker, biological molecule found in body fluids (cf. blood, urine) or tissues that may signal an abnormal physiological condition or disease; hormone, chemical messenger of the endocrine system; neurotransmitter, chemical messenger of the nervous system; enzyme, biomolecular catalyst enabling a specific chemical reaction; labeled detection, target biomolecule detection by attaching a secondary molecule ("tag") that can be readily detected through its intrinsic properties, most commonly fluorescence, also magnetic, electrochemical, etc.; label-free detection, direct target biomolecule detection based on its properties (such as optical absorption, electrical conductivity, etc.) without the use of a tag.

■ REFERENCES

(1) Roy, J. *Response of plants to multiple stresses*; Academic Press: 2012.

(2) Chrousos, G. P. Stress and disorders of the stress system. *Nat. Rev. Endocrinol.* **2009**, *5* (7), 374−381.

(3) Horowitz, M. J. *Stress response syndromes: PTSD, grief, and adjustment disorders*; Jason Aronson: 1997.

(4) Everly, G. S., Jr; Lating, J. M. *A clinical guide to the treatment of the human stress response*; Springer Science & Business Media: 2012.

(5) Nater, U. M.; Skoluda, N.; Strahler, J. Biomarkers of stress in behavioural medicine. *Current opinion in psychiatry* **2013**, *26* (5), 440−445.

(6) FDA-NIH Biomarker Working Group *BEST (biomarkers, endpoints, and other tools) resource*; 2016.

(7) Charmandari, E.; Tsigos, C.; Chrousos, G. Endocrinology of the stress response. *Annu. Rev. Physiol.* **2005**, *67*, 259−284.

(8) Ulrich-Lai, Y. M.; Herman, J. P. Neural regulation of endocrine and autonomic stress responses. *Nat. Rev. Neurosci.* **2009**, *10* (6), 397−409.

(9) Pruessner, J. C.; Dedovic, K.; Pruessner, M.; Lord, C.; Buss, C.; Collins, L.; Dagher, A.; Lupien, S. J. Stress regulation in the central nervous system: evidence from structural and functional neuroimaging studies in human populations-2008 Curt Richter Award Winner. *Psychoneuroendocrinology* **2010**, *35* (1), 179−191.

(10) Ritvanen, T.; Louhevaara, V.; Helin, P.; Väisänen, S.; Hänninen, O. Responses of the autonomic nervous system during periods of perceived high and low work stress in younger and older female teachers. *Applied Ergonomics* **2006**, *37* (3), 311−318.

(11) Saladin, K. S.; Miller, L. *Anatomy & physiology*; WCB/McGraw-Hill: New York, 1998.

(12) Silverthorn, D. U.; Ober, W. C.; Garrison, C. W.; Silverthorn, A. C.; Johnson, B. R. *Human physiology: an integrated approach*; Pearson/Benjamin Cummings: San Francisco, CA, 2009.

(13) Kohrle, J.; Jakob, F.; Contempre, B.; Dumont, J. E. Selenium, the thyroid, and the endocrine system. *Endocr. Rev.* **2005**, *26* (7), 944−984.

(14) Goldstein, D. S. Adrenal responses to stress. *Cell. Mol. Neurobiol.* **2010**, *30* (8), 1433−1440.

(15) Scott, J. D.; Pawson, T. Cell communication: The inside story. *Sci. Am.* **2000**, *282* (6), 72−79.

(16) Westphal, U. Steroid-protein interactions revisited. In *Steroid-Protein Interactions II*; Springer: 1986; pp 1−7.

(17) Cooper, G. The Cell: A Molecular Approach, 2nd edn. *The Cell: A Molecular Approach*; Sinauer Associates, Sunderland, MA: 2000.

(18) Aranda, A.; Pascual, A. Nuclear hormone receptors and gene expression. *Physiol. Rev.* **2001**, *81* (3), 1269−1304.

(19) Banks, W. A.; Kastin, A. J. Peptides and the blood-brain barrier: lipophilicity as a predictor of permeability. *Brain Res. Bull.* **1985**, *15* (3), 287−292.

(20) Chawla, A.; Repa, J. J.; Evans, R. M.; Mangelsdorf, D. J. Nuclear receptors and lipid physiology: opening the X-files. *Science* **2001**, *294* (5548), 1866−1870.

DOI: 10.1021/acssensors.8b00726
ACS Sens. 2018, 3, 2025−2044

(21) Green, S.; Chambon, P. Nuclear receptors enhance our understanding of transcription regulation. *Trends Genet.* **1988**, *4* (11), 309−314.
(22) Mai, J. K.; Paxinos, G. *The human nervous system*; Academic Press: 2011.
(23) Solms, M.; Turnbull, O. *The brain and the inner world: An introduction to the neuroscience of subjective experience*; Karnac Books: 2002.
(24) Kandel, E. R.; Schwartz, J. H.; Jessell, T. M.; Siegelbaum, S. A.; Hudspeth, A. J. *Principles of neural science*; McGraw-Hill: New York, 2000; Vol. *4*.
(25) Newman, E. A. New roles for astrocytes: regulation of synaptic transmission. *Trends Neurosci.* **2003**, *26* (10), 536−542.
(26) Agnati, L.; Zoli, M.; Strömberg, I.; Fuxe, K. Intercellular communication in the brain: wiring versus volume transmission. *Neuroscience* **1995**, *69* (3), 711−726.
(27) Calabrese, F.; Molteni, R.; Racagni, G.; Riva, M. A. Neuronal plasticity: a link between stress and mood disorders. *Psychoneuroendocrinology* **2009**, *34*, S208−S216.
(28) Webster, R. *Neurotransmitters, drugs and brain function*; John Wiley & Sons: 2001.
(29) Rohleder, N.; Nater, U. M.; Wolf, J. M.; Ehlert, U.; Kirschbaum, C. Psychosocial stress-induced activation of salivary alpha-amylase: an indicator of sympathetic activity? *Ann. N. Y. Acad. Sci.* **2004**, *1032* (1), 258−263.
(30) Toy, R.; Hayden, E.; Shoup, C.; Baskaran, H.; Karathanasis, E. The effects of particle size, density and shape on margination of nanoparticles in microcirculation. *Nanotechnology* **2011**, *22* (11), 115101.
(31) Cheng, S.; Shi, F.; Jiang, X.; Wang, L.; Chen, W.; Zhu, C. Sensitive detection of small molecules by competitive immunomagnetic-proximity ligation assay. *Anal. Chem.* **2012**, *84* (5), 2129−2132.
(32) Du, P.; Jin, M.; Chen, G.; Zhang, C.; Jiang, Z.; Zhang, Y.; Zou, P.; She, Y.; Jin, F.; Shao, H.; et al. A Competitive Bio-Barcode Amplification Immunoassay for Small Molecules Based on Nanoparticles. *Sci. Rep.* **2016**, *6*, 38114.
(33) Lipinski, C. A.; Lombardo, F.; Dominy, B. W.; Feeney, P. J. Experimental and computational approaches to estimate solubility and permeability in drug discovery and development settings. *Adv. Drug Delivery Rev.* **1997**, *23* (1−3), 3−25.
(34) Rifai, N.; Gillette, M. A.; Carr, S. A. Protein biomarker discovery and validation: the long and uncertain path to clinical utility. *Nat. Biotechnol.* **2006**, *24* (8), 971−983.
(35) Li, H.; Rothberg, L. Colorimetric detection of DNA sequences based on electrostatic interactions with unmodified gold nanoparticles. *Proc. Natl. Acad. Sci. U. S. A.* **2004**, *101* (39), 14036−14039.
(36) Wei, F.; Patel, P.; Liao, W.; Chaudhry, K.; Zhang, L.; Arellano-Garcia, M.; Hu, S.; Elashoff, D.; Zhou, H.; Shukla, S.; et al. Electrochemical sensor for multiplex biomarkers detection. *Clin. Cancer Res.* **2009**, *15* (13), 4446−4452.
(37) Sun, K.; Ramgir, N.; Bhansali, S. An immunoelectrochemical sensor for salivary cortisol measurement. *Sens. Actuators, B* **2008**, *133* (2), 533−537.
(38) Wang, M.; You, J. Mass spectrometry for protein quantification in biomarker discovery. *Methods Mol. Biol.* **2012**, *815*, 199−225.
(39) Rose, R.; Kreuz, L.; Holaday, J.; Sulak, K.; Johnson, C. Diurnal variation of plasma testosterone and cortisol. *J. Endocrinol.* **1972**, *54* (1), 177−178.
(40) Matchock, R. L.; Dorn, L. D.; Susman, E. J. Diurnal and seasonal cortisol, testosterone, and DHEA rhythms in boys and girls during puberty. *Chronobiol. Int.* **2007**, *24* (5), 969−990.
(41) Rusling, J. F.; Kumar, C. V.; Gutkind, J. S.; Patel, V. Measurement of biomarker proteins for point-of-care early detection and monitoring of cancer. *Analyst* **2010**, *135* (10), 2496−2511.
(42) Pereira, L.; Souza, R. D.; Orlande, H.; Cotta, R. A comparison of concentration measurement techniques for the estimation of the apparent mass diffusion coefficient. *Braz. J. Chem. Eng.* **2001**, *18* (3), 253−265.
(43) Jia, M.; Chew, W. M.; Feinstein, Y.; Skeath, P.; Sternberg, E. M. Quantification of cortisol in human eccrine sweat by liquid chromatography−tandem mass spectrometry. *Analyst* **2016**, *141* (6), 2053−2060.
(44) Granger, D. A.; Kivlighan, K. T.; El-SHEIKH, M.; Gordis, E. B.; Stroud, L. R. Salivary α-amylase in biobehavioral research. *Ann. N. Y. Acad. Sci.* **2007**, *1098* (1), 122−144.
(45) Noble, R. E. Salivary α-amylase and lysozyme levels: A non-invasive technique for measuring parotid vs submandibular/sublingual gland activity. *J. Oral Sci.* **2000**, *42* (2), 83−86.
(46) Sahu, G. K.; Upadhyay, S.; Panna, S. M. Salivary alpha amylase activity in human beings of different age groups subjected to psychological stress. *Indian J. Clin. Biochem.* **2014**, *29* (4), 485−490.
(47) Nater, U. M.; Rohleder, N. Salivary alpha-amylase as a non-invasive biomarker for the sympathetic nervous system: current state of research. *Psychoneuroendocrinology* **2009**, *34* (4), 486−496.
(48) Lommatzsch, M.; Zingler, D.; Schuhbaeck, K.; Schloetcke, K.; Zingler, C.; Schuff-Werner, P.; Virchow, J. C. The impact of age, weight and gender on BDNF levels in human platelets and plasma. *Neurobiol. Aging* **2005**, *26* (1), 115−123.
(49) Brierley, G.; Priebe, I.; Purins, L.; Fung, K.; Tabor, B.; Lockett, T.; Nice, E.; Gibbs, P.; Tie, J.; McMurrick, P.; et al. Serum concentrations of brain-derived neurotrophic factor (BDNF) are decreased in colorectal cancer patients. *Cancer Biomarkers* **2012**, *13* (2), 67−73.
(50) Suliman, S.; Hemmings, S. M.; Seedat, S. Brain-Derived Neurotrophic Factor (BDNF) protein levels in anxiety disorders: systematic review and meta-regression analysis. *Front. Integr. Neurosci.* **2013**, *7*, 55.
(51) Lee, B.-H.; Kim, Y.-K. The roles of BDNF in the pathophysiology of major depression and in antidepressant treatment. *Psychiatry Invest.* **2010**, *7* (4), 231−235.
(52) Mandel, A. L.; Ozdener, H.; Utermohlen, V. Brain-derived neurotrophic factor in human saliva: ELISA optimization and biological correlates. *J. Immunoassay Immunochem.* **2011**, *32* (1), 18−30.
(53) McMorris, T.; Swain, J.; Smith, M.; Corbett, J.; Delves, S.; Sale, C.; Harris, R. C.; Potter, J. Heat stress, plasma concentrations of adrenaline, noradrenaline, 5-hydroxytryptamine and cortisol, mood state and cognitive performance. *International Journal of Psychophysiology* **2006**, *61* (2), 204−215.
(54) Le Roux, C. W.; Sivakumaran, S.; Alaghband-Zadeh, J.; Dhillo, W.; Kong, W. M.; Wheeler, M. J. Free cortisol index as a surrogate marker for serum free cortisol. *Ann. Clin. Biochem.* **2002**, *39* (4), 406−408.
(55) Hellhammer, D. H.; Wüst, S.; Kudielka, B. M. Salivary cortisol as a biomarker in stress research. *Psychoneuroendocrinology* **2009**, *34* (2), 163−171.
(56) Cohen, J.; Deans, R.; Dalley, A.; Lipman, J.; Roberts, M. S.; Venkatesh, B. Measurement of tissue cortisol levels in patients with severe burns: a preliminary investigation. *Critical Care* **2009**, *13* (6), R189.
(57) Venugopal, M.; Arya, S. K.; Chornokur, G.; Bhansali, S. A realtime and continuous assessment of cortisol in ISF using electrochemical impedance spectroscopy. *Sens. Actuators, A* **2011**, *172* (1), 154−160.
(58) Sakihara, S.; Kageyama, K.; Oki, Y.; Doi, M.; Iwasaki, Y.; Takayasu, S.; Moriyama, T.; Terui, K.; Nigawara, T.; Hirata, Y.; et al. Evaluation of plasma, salivary, and urinary cortisol levels for diagnosis of Cushing's syndrome. *Endocr. J.* **2010**, *57* (4), 331−337.
(59) Venge, P.; Johnston, N.; Lindahl, B.; James, S. Normal plasma levels of cardiac troponin I measured by the high-sensitivity cardiac troponin I access prototype assay and the impact on the diagnosis of myocardial ischemia. *J. Am. Coll. Cardiol.* **2009**, *54* (13), 1165−1172.
(60) Araújo, K.; da Silva, J.; Sañudo, A.; Kopelman, B. Plasma concentrations of cardiac troponin I in newborn infants. *Clin. Chem.* **2004**, *50* (9), 1717−1718.
(61) Mizrahi, R.; Addington, J.; Rusjan, P. M.; Suridjan, I.; Ng, A.; Boileau, I.; Pruessner, J. C.; Remington, G.; Houle, S.; Wilson, A. A.

DOI: 10.1021/acssensors.8b00726
ACS Sens. 2018, 3, 2025−2044

Increased stress-induced dopamine release in psychosis. *Biol. Psychiatry* **2012**, *71* (6), 561−567.
(62) Davidson, D. F. Elevated urinary dopamine in adults and children. *Ann. Clin. Biochem.* **2005**, *42* (3), 200−207.
(63) Ambade, V.; Arora, M.; Singh, P.; Somani, B.; Basannar, D. Adrenaline, noradrenaline and dopamine level estimation in depression: Does it help? *Medical Journal Armed Forces India* **2009**, *65* (3), 216−220.
(64) Dodt, C.; Breckling, U.; Derad, I.; Fehm, H. L.; Born, J. Plasma epinephrine and norepinephrine concentrations of healthy humans associated with nighttime sleep and morning arousal. *Hypertension* **1997**, *30* (1), 71−76.
(65) Fan, W.; Liu, X.; Yue, J. Determination of urine tumor necrosis factor, IL-6, IL-8, and serum IL-6 in patients with hemorrhagic fever with renal syndrome. *Braz. J. Infect. Dis.* **2012**, *16* (6), 527−530.
(66) Munge, B. S.; Krause, C. E.; Malhotra, R.; Patel, V.; Gutkind, J. S.; Rusling, J. F. Electrochemical immunosensors for interleukin-6. Comparison of carbon nanotube forest and gold nanoparticle platforms. *Electrochem. Commun.* **2009**, *11* (5), 1009−1012.
(67) Iwase, S.; Murakami, T.; Saito, Y.; Nakagawa, K. Steep elevation of blood interleukin-6 (IL-6) associated only with late stages of cachexia in cancer patients. *Eur. Cytokine Network* **2004**, *15* (4), 312−316.
(68) Luft, F.; Rankin, L.; Henry, D.; Bloch, R.; Grim, C.; Weyman, A.; Murray, R.; Weinberger, M. Plasma and urinary norepinephrine values at extremes of sodium intake in normal man. *Hypertension* **1979**, *1* (3), 261−266.
(69) Xing, J.; Koba, S.; Kehoe, V.; Gao, Z.; Rice, K.; King, N.; Sinoway, L.; Li, J. Interstitial norepinephrine concentrations in skeletal muscle of ischemic heart failure. *American Journal of Physiology-Heart and Circulatory Physiology* **2007**, *293* (2), H1190−H1195.
(70) Mortensen, S. P.; González-Alonso, J.; Nielsen, J.-J.; Saltin, B.; Hellsten, Y. Muscle interstitial ATP and norepinephrine concentrations in the human leg during exercise and ATP infusion. *J. Appl. Physiol.* **2009**, *107* (6), 1757−1762.
(71) Pietrzak, R. H.; Gallezot, J.-D.; Ding, Y.-S.; Henry, S.; Potenza, M. N.; Southwick, S. M.; Krystal, J. H.; Carson, R. E.; Neumeister, A. Association of posttraumatic stress disorder with reduced in vivo norepinephrine transporter availability in the locus coeruleus. *JAMA Psychiatry* **2013**, *70* (11), 1199−1205.
(72) Kuo, L. E.; Zukowska, Z. Stress, NPY and vascular remodeling: Implications for stress-related diseases. *Peptides* **2007**, *28* (2), 435−440.
(73) Rasmusson, A. M.; Southwick, S. M.; Hauger, R. L.; Charney, D. S. Plasma neuropeptide Y (NPY) increases in humans in response to the α2 antagonist yohimbine. *Neuropsychopharmacology* **1998**, *19* (1), 95−98.
(74) Morgan, C. A.; Rasmusson, A. M.; Wang, S.; Hoyt, G.; Hauger, R. L.; Hazlett, G. Neuropeptide-Y, cortisol, and subjective distress in humans exposed to acute stress: replication and extension of previous report. *Biol. Psychiatry* **2002**, *52* (2), 136−142.
(75) Tu, C.; Zhao, D.; Lin, X. Levels of neuropeptide-Y in the plasma and skin tissue fluids of patients with vitiligo. *J. Dermatol. Sci.* **2001**, *27* (3), 178−182.
(76) Igarashi, N.; Tatsumi, K.; Nakamura, A.; Sakao, S.; Takiguchi, Y.; Nishikawa, T.; Kuriyama, T. Plasma orexin-A levels in obstructive sleep apnea-hypopnea syndrome. *Chest* **2003**, *124* (4), 1381−1385.
(77) Kastin, A. J.; Akerstrom, V. Orexin A but not orexin B rapidly enters brain from blood by simple diffusion. *J. Pharmacol. Exp. Ther.* **1999**, *289* (1), 219−223.
(78) Cun, Y.; Tang, L.; Yan, J.; He, C.; Li, Y.; Hu, Z.; Xia, J. Orexin A attenuates the sleep-promoting effect of adenosine in the lateral hypothalamus of rats. *Neurosci. Bull.* **2014**, *30* (5), 877−886.
(79) Humble, M. B.; Uvnäs-Moberg, K.; Engström, I.; Bejerot, S. Plasma oxytocin changes and anti-obsessive response during serotonin reuptake inhibitor treatment: a placebo controlled study. *BMC Psychiatry* **2013**, *13* (1), 344.
(80) Reyes, T. L.; Galinsky, A. M.; Hoffmann, J. N.; You, H. M.; Ziegler, T. E.; McClintock, M. K. Social Peptides: Measuring Urinary Oxytocin and Vasopressin in a Home Field Study of Older Adults at Risk for Dehydration. *J. Gerontol., Ser. B* **2014**, *69* (Suppl 2), S229−S237.
(81) Kema, I. P.; De Vries, E.; Slooff, M.; Biesma, B.; Muskiet, F. Serotonin, catecholamines, histamine, and their metabolites in urine, platelets, and tumor tissue of patients with carcinoid tumors. *Clin. Chem.* **1994**, *40* (1), 86−95.
(82) Chaouloff, F.; Berton, O.; Mormède, P. Serotonin and stress. *Neuropsychopharmacology* **1999**, *21*, 28S−32S.
(83) Chaouloff, F. Serotonin, stress and corticoids. *J. Psychopharmacol.* **2000**, *14* (2), 139−151.
(84) Berndt, T. J.; Liang, M.; Tyce, G. M.; Knox, F. G. Intrarenal serotonin, dopamine, and phosphate handling in remnant kidneys. *Kidney Int.* **2001**, *59* (2), 625−630.
(85) Nakai, Y.; Hamagaki, S.; Takagi, R.; Taniguchi, A.; Kurimoto, F. Plasma Concentrations of Tumor Necrosis Factor-α (TNF-α) and Soluble TNF Receptors in Patients with Anorexia Nervosa 1. *J. Clin. Endocrinol. Metab.* **1999**, *84* (4), 1226−1228.
(86) Zhang, A.; Sun, H.; Yan, G.; Wang, P.; Wang, X. Mass spectrometry-based metabolomics: applications to biomarker and metabolic pathway research. *Biomed. Chromatogr.* **2016**, *30* (1), 7−12.
(87) Gika, H. G.; Theodoridis, G. A.; Plumb, R. S.; Wilson, I. D. Current practice of liquid chromatography−mass spectrometry in metabolomics and metabonomics. *J. Pharm. Biomed. Anal.* **2014**, *87*, 12−25.
(88) Saliterman, S. S. *Fundamentals of BioMEMS and Medical Microdevices*; Wiley-Interscience: Bellingham, WA, 2006.
(89) Vashist, S. K.; Luppa, P. B.; Yeo, L. Y.; Ozcan, A.; Luong, J. H. Emerging technologies for next-generation point-of-care testing. *Trends Biotechnol.* **2015**, *33* (11), 692−705.
(90) Song, Y.; Huang, Y.-Y.; Liu, X.; Zhang, X.; Ferrari, M.; Qin, L. Point-of-care technologies for molecular diagnostics using a drop of blood. *Trends Biotechnol.* **2014**, *32* (3), 132−139.
(91) Agarwal, A.; Lang, J. *Foundations of Analog and Digital Electronic Circuits*; Elsevier: 2005.
(92) Qureshi, A.; Gurbuz, Y.; Niazi, J. H. Biosensors for cardiac biomarkers detection: a review. *Sens. Actuators, B* **2012**, *171*, 62−76.
(93) Meninger, S.; Mur-Miranda, J. O.; Amirtharajah, R.; Chandrakasan, A.; Lang, J. H. Vibration-to-electric energy conversion. *IEEE Transactions on Very Large Scale Integration (VLSI) Systems* **2001**, *9* (1), 64−76.
(94) Jung, W.; Han, J.; Choi, J.-W.; Ahn, C. H. Point-of-care testing (POCT) diagnostic systems using microfluidic lab-on-a-chip technologies. *Microelectron. Eng.* **2015**, *132*, 46−57.
(95) Choi, D. H.; Lee, S. K.; Oh, Y. K.; Bae, B. W.; Lee, S. D.; Kim, S.; Shin, Y.-B.; Kim, M.-G. A dual gold nanoparticle conjugate-based lateral flow assay (LFA) method for the analysis of troponin I. *Biosens. Bioelectron.* **2010**, *25* (8), 1999−2002.
(96) Guo, X. Surface plasmon resonance based biosensor technique: a review. *J. Biophotonics* **2012**, *5* (7), 483−501.
(97) Malhotra, R.; Patel, V.; Vaqué, J. P.; Gutkind, J. S.; Rusling, J. F. Ultrasensitive electrochemical immunosensor for oral cancer biomarker IL-6 using carbon nanotube forest electrodes and multilabel amplification. *Anal. Chem.* **2010**, *82* (8), 3118−3123.
(98) Xu, Y.; Liu, Y.; Wu, Y.; Xia, X.; Liao, Y.; Li, Q. Fluorescent probe-based lateral flow assay for multiplex nucleic acid detection. *Anal. Chem.* **2014**, *86* (12), 5611−5614.
(99) Mirasoli, M.; Buragina, A.; Dolci, L. S.; Simoni, P.; Anfossi, L.; Giraudi, G.; Roda, A. Chemiluminescence-based biosensor for fumonisins quantitative detection in maize samples. *Biosens. Bioelectron.* **2012**, *32* (1), 283−287.
(100) Posthuma-Trumpie, G. A.; Korf, J.; van Amerongen, A. Lateral flow (immuno) assay: its strengths, weaknesses, opportunities and threats. A literature survey. *Anal. Bioanal. Chem.* **2009**, *393* (2), 569−582.

DOI: 10.1021/acssensors.8b00726
ACS Sens. 2018, 3, 2025−2044

(101) Sajid, M.; Kawde, A.-N.; Daud, M. Designs, formats and applications of lateral flow assay: A literature review. *J. Saudi Chem. Soc.* **2015**, *19* (6), 689−705.
(102) Li, Z.; Wang, Y.; Wang, J.; Tang, Z.; Pounds, J. G.; Lin, Y. Rapid and sensitive detection of protein biomarker using a portable fluorescence biosensor based on quantum dots and a lateral flow test strip. *Anal. Chem.* **2010**, *82* (16), 7008−7014.
(103) Chong, H.; Koo, Y.; Collins, B.; Gomez, F.; Yun, Y.; Sankar, J. Paper-based microfluidic point-of-care diagnostic devices for monitoring drug metabolism. *J. Nanomed. Biother. Discovery* **2013**, *3*, e122.
(104) Wang, S.; Chinnasamy, T.; Lifson, M. A.; Inci, F.; Demirci, U. Flexible substrate-based devices for point-of-care diagnostics. *Trends Biotechnol.* **2016**, *34* (11), 909−921.
(105) Cheng, C.-M.; Kuan, C.-M.; Chen, C.-F. Polymeric-Based In Vitro Diagnostic Devices. In *In-Vitro Diagnostic Devices*; Springer: 2016; pp 15−58.
(106) Focke, M.; Kosse, D.; Müller, C.; Reinecke, H.; Zengerle, R.; von Stetten, F. Lab-on-a-Foil: microfluidics on thin and flexible films. *Lab Chip* **2010**, *10* (11), 1365−1386.
(107) Yetisen, A. K.; Montelongo, Y.; da Cruz Vasconcellos, F.; Martinez-Hurtado, J.; Neupane, S.; Butt, H.; Qasim, M. M.; Blyth, J.; Burling, K.; Carmody, J. B.; et al. Reusable, robust, and accurate laser-generated photonic nanosensor. *Nano Lett.* **2014**, *14* (6), 3587−3593.
(108) Tokel, O.; Yildiz, U. H.; Inci, F.; Durmus, N. G.; Ekiz, O. O.; Turker, B.; Cetin, C.; Rao, S.; Sridhar, K.; Natarajan, N.; et al. Portable microfluidic integrated plasmonic platform for pathogen detection. *Sci. Rep.* **2015**, *5*, 9152.
(109) Holden, M. T.; Carter, M. C.; Wu, C.-H.; Wolfer, J.; Codner, E.; Sussman, M. R.; Lynn, D. M.; Smith, L. M. Photolithographic synthesis of high-density DNA and RNA arrays on flexible, transparent, and easily subdivided plastic substrates. *Anal. Chem.* **2015**, *87* (22), 11420−11428.
(110) Tee, B. C.; Wang, C.; Allen, R.; Bao, Z. An electrically and mechanically self-healing composite with pressure-and flexion-sensitive properties for electronic skin applications. *Nat. Nanotechnol.* **2012**, *7* (12), 825−832.
(111) Pang, C.; Lee, C.; Suh, K. Y. Recent advances in flexible sensors for wearable and implantable devices. *J. Appl. Polym. Sci.* **2013**, *130* (3), 1429−1441.
(112) Arlett, J.; Myers, E.; Roukes, M. Comparative advantages of mechanical biosensors. *Nat. Nanotechnol.* **2011**, *6* (4), 203−215.
(113) Nair, P. R.; Alam, M. A. Design considerations of silicon nanowire biosensors. *IEEE Trans. Electron Devices* **2007**, *54* (12), 3400−3408.
(114) Schmidt, C.; Mayer, M.; Vogel, H. A chip-based biosensor for the functional analysis of single ion channels. *Angew. Chem., Int. Ed.* **2000**, *39* (17), 3137−3140.
(115) Harraz, F. A. Porous silicon chemical sensors and biosensors: A review. *Sens. Actuators, B* **2014**, *202*, 897−912.
(116) Dhanekar, S.; Jain, S. Porous silicon biosensor: current status. *Biosens. Bioelectron.* **2013**, *41*, 54−64.
(117) Rossi, A. M.; Wang, L.; Reipa, V.; Murphy, T. E. Porous silicon biosensor for detection of viruses. *Biosens. Bioelectron.* **2007**, *23* (5), 741−745.
(118) Xia, F.; Zuo, X.; Yang, R.; Xiao, Y.; Kang, D.; Vallée-Bélisle, A.; Gong, X.; Yuen, J. D.; Hsu, B. B.; Heeger, A. J.; et al. Colorimetric detection of DNA, small molecules, proteins, and ions using unmodified gold nanoparticles and conjugated polyelectrolytes. *Proc. Natl. Acad. Sci. U. S. A.* **2010**, *107* (24), 10837−10841.
(119) Ohno, R.; Ohnuki, H.; Wang, H.; Yokoyama, T.; Endo, H.; Tsuya, D.; Izumi, M. Electrochemical impedance spectroscopy biosensor with interdigitated electrode for detection of human immunoglobulin A. *Biosens. Bioelectron.* **2013**, *40* (1), 422−426.
(120) Lisdat, F.; Schäfer, D. The use of electrochemical impedance spectroscopy for biosensing. *Anal. Bioanal. Chem.* **2008**, *391* (5), 1555.
(121) Chang, B.-Y.; Park, S.-M. Electrochemical impedance spectroscopy. *Annu. Rev. Anal. Chem.* **2010**, *3*, 207−229.
(122) Kaushik, A.; Yndart, A.; Jayant, R. D.; Sagar, V.; Atluri, V.; Bhansali, S.; Nair, M. Electrochemical sensing method for point-of-care cortisol detection in human immunodeficiency virus-infected patients. *Int. J. Nanomed.* **2015**, *10*, 677−685.
(123) Zhuo, Y.; Chai, Y.-Q.; Yuan, R.; Mao, L.; Yuan, Y.-L.; Han, J. Glucose oxidase and ferrocene labels immobilized at Au/TiO 2 nanocomposites with high load amount and activity for sensitive immunoelectrochemical measurement of ProGRP biomarker. *Biosens. Bioelectron.* **2011**, *26* (9), 3838−3844.
(124) Buss, H.; Chan, T. P.; Sluis, K. B.; Domigan, N. M.; Winterbourn, C. C. Protein carbonyl measurement by a sensitive ELISA method. *Free Radical Biol. Med.* **1997**, *23* (3), 361−366.
(125) Alamdari, D. H.; Kostidou, E.; Paletas, K.; Sarigianni, M.; Konstas, A. G.; Karapiperidou, A.; Koliakos, G. High sensitivity enzyme-linked immunosorbent assay (ELISA) method for measuring protein carbonyl in samples with low amounts of protein. *Free Radical Biol. Med.* **2005**, *39* (10), 1362−1367.
(126) Wang, S.; Zhang, Q.; Wang, R.; Yoon, S. A novel multi-walled carbon nanotube-based biosensor for glucose detection. *Biochem. Biophys. Res. Commun.* **2003**, *311* (3), 572−576.
(127) Kleiren, E.; Ruysschaert, J.-M.; Goormaghtigh, E.; Raussens, V. Development of a quantitative and conformation-sensitive ATR-FTIR biosensor for Alzheimer's disease: The effect of deuteration on the detection of the Aβ peptide. *Spectroscopy* **2010**, *24* (1−2), 61−66.
(128) Gupta, V. K.; Yola, M. L.; Qureshi, M. S.; Solak, A. O.; Atar, N.; Üstündağ, Z. A novel impedimetric biosensor based on graphene oxide/gold nanoplatform for detection of DNA arrays. *Sens. Actuators, B* **2013**, *188*, 1201−1211.
(129) Rushworth, J. V.; Ahmed, A.; Griffiths, H. H.; Pollock, N. M.; Hooper, N. M.; Millner, P. A. A label-free electrical impedimetric biosensor for the specific detection of Alzheimer's amyloid-beta oligomers. *Biosens. Bioelectron.* **2014**, *56*, 83−90.
(130) O'Farrell, B. Evolution in lateral flow−based immunoassay systems. In *Lateral flow immunoassay*; Springer: 2009; pp 1−33.
(131) Domon, B.; Aebersold, R. Mass spectrometry and protein analysis. *Science* **2006**, *312* (5771), 212−217.
(132) Pitt, J. J. Principles and applications of liquid chromatography-mass spectrometry in clinical biochemistry. *Clin. Biochem. Rev.* **2009**, *30* (1), 19−34.
(133) Lee, H.; Sun, E.; Ham, D.; Weissleder, R. Chip−NMR biosensor for detection and molecular analysis of cells. *Nat. Med.* **2008**, *14* (8), 869−874.
(134) Roy, V.; Brotin, T.; Dutasta, J. P.; Charles, M. H.; Delair, T.; Mallet, F.; Huber, G.; Desvaux, H.; Boulard, Y.; Berthault, P. A cryptophane biosensor for the detection of specific nucleotide targets through xenon NMR spectroscopy. *ChemPhysChem* **2007**, *8* (14), 2082−2085.
(135) Oncescu, V.; O'Dell, D.; Erickson, D. Smartphone based health accessory for colorimetric detection of biomarkers in sweat and saliva. *Lab Chip* **2013**, *13* (16), 3232−3238.
(136) Piliarik, M.; Vaisocherová, H.; Homola, J. Surface plasmon resonance biosensing. *Biosensors and Biodetection* **2009**, *503*, 65−88.
(137) Rich, R. L.; Myszka, D. G. Advances in surface plasmon resonance biosensor analysis. *Curr. Opin. Biotechnol.* **2000**, *11* (1), 54−61.
(138) Anker, J. N.; Hall, W. P.; Lyandres, O.; Shah, N. C.; Zhao, J.; Van Duyne, R. P. Biosensing with plasmonic nanosensors. In *Nanoscience and Technology: A Collection of Reviews from Nature Journals*; World Scientific: 2010; pp 308−319.
(139) Kan, J.; Pan, X.; Chen, C. Polyaniline−uricase biosensor prepared with template process. *Biosens. Bioelectron.* **2004**, *19* (12), 1635−1640.
(140) Chen, K.-J.; Lee, C.-F.; Rick, J.; Wang, S.-H.; Liu, C.-C.; Hwang, B.-J. Fabrication and application of amperometric glucose biosensor based on a novel PtPd bimetallic nanoparticle decorated multi-walled carbon nanotube catalyst. *Biosens. Bioelectron.* **2012**, *33* (1), 75−81.

DOI: 10.1021/acssensors.8b00726
ACS Sens. 2018, 3, 2025−2044

(141) Kolmakov, A.; Zhang, Y.; Cheng, G.; Moskovits, M. Detection of CO and O2 using tin oxide nanowire sensors. *Adv. Mater.* **2003**, *15* (12), 997−1000.
(142) Georganopoulou, D. G.; Chang, L.; Nam, J.-M.; Thaxton, C. S.; Mufson, E. J.; Klein, W. L.; Mirkin, C. A. Nanoparticle-based detection in cerebral spinal fluid of a soluble pathogenic biomarker for Alzheimer's disease. *Proc. Natl. Acad. Sci. U. S. A.* **2005**, *102* (7), 2273−2276.
(143) Liu, X.; Dai, Q.; Austin, L.; Coutts, J.; Knowles, G.; Zou, J.; Chen, H.; Huo, Q. A one-step homogeneous immunoassay for cancer biomarker detection using gold nanoparticle probes coupled with dynamic light scattering. *J. Am. Chem. Soc.* **2008**, *130* (9), 2780−2782.
(144) Arya, S. K.; Chornokur, G.; Venugopal, M.; Bhansali, S. Antibody functionalized interdigitated μ-electrode (IDμE) based impedimetric cortisol biosensor. *Analyst* **2010**, *135* (8), 1941−1946.
(145) Zangheri, M.; Cevenini, L.; Anfossi, L.; Baggiani, C.; Simoni, P.; Di Nardo, F.; Roda, A. A simple and compact smartphone accessory for quantitative chemiluminescence-based lateral flow immunoassay for salivary cortisol detection. *Biosens. Bioelectron.* **2015**, *64*, 63−68.
(146) Sanghavi, B. J.; Moore, J. A.; Chávez, J. L.; Hagen, J. A.; Kelley-Loughnane, N.; Chou, C.-F.; Swami, N. S. Aptamer-functionalized nanoparticles for surface immobilization-free electrochemical detection of cortisol in a microfluidic device. *Biosens. Bioelectron.* **2016**, *78*, 244−252.
(147) Kumar, A.; Aravamudhan, S.; Gordic, M.; Bhansali, S.; Mohapatra, S. S. Ultrasensitive detection of cortisol with enzyme fragment complementation technology using functionalized nanowire. *Biosens. Bioelectron.* **2007**, *22* (9−10), 2138−2144.
(148) Carrozza, C.; Corsello, S. M.; Paragliola, R. M.; Ingraudo, F.; Palumbo, S.; Locantore, P.; Sferrazza, A.; Pontecorvi, A.; Zuppi, C. Clinical accuracy of midnight salivary cortisol measured by automated electrochemiluminescence immunoassay method in Cushing's syndrome. *Ann. Clin. Biochem.* **2010**, *47* (3), 228−232.
(149) Stevens, R. C.; Soelberg, S. D.; Near, S.; Furlong, C. E. Detection of cortisol in saliva with a flow-filtered, portable surface plasmon resonance biosensor system. *Anal. Chem.* **2008**, *80* (17), 6747−6751.
(150) Yamaguchi, M.; Matsuda, Y.; Sasaki, S.; Sasaki, M.; Kadoma, Y.; Imai, Y.; Niwa, D.; Shetty, V. Immunosensor with fluid control mechanism for salivary cortisol analysis. *Biosens. Bioelectron.* **2013**, *41*, 186−191.
(151) Tuteja, S. K.; Ormsby, C.; Neethirajan, S. Noninvasive Label-Free Detection of Cortisol and Lactate Using Graphene Embedded Screen-Printed Electrode. *Nano-Micro Lett.* **2018**, *10* (3), 41.
(152) Munje, R. D.; Muthukumar, S.; Selvam, A. P.; Prasad, S. Flexible nanoporous tunable electrical double layer biosensors for sweat diagnostics. *Sci. Rep.* **2015**, *5*, 14586.
(153) Jagadeesan, K. K.; Kumar, S.; Sumana, G. Application of conducting paper for selective detection of troponin. *Electrochem. Commun.* **2012**, *20*, 71−74.
(154) Dittmer, W. U.; Evers, T. H.; Hardeman, W. M.; Huijnen, W.; Kamps, R.; de Kievit, P.; Neijzen, J. H.; Nieuwenhuis, J. H.; Sijbers, M. J.; Dekkers, D. W.; et al. Rapid, high sensitivity, point-of-care test for cardiac troponin based on optomagnetic biosensor. *Clin. Chim. Acta* **2010**, *411* (11−12), 868−873.
(155) de Vasconcelos, E. A.; Peres, N. G.; Pereira, C. O.; da Silva, V. L.; da Silva, E. F., Jr; Dutra, R. F. Potential of a simplified measurement scheme and device structure for a low cost label-free point-of-care capacitive biosensor. *Biosens. Bioelectron.* **2009**, *25* (4), 870−876.
(156) Kong, T.; Su, R.; Zhang, B.; Zhang, Q.; Cheng, G. CMOS-compatible, label-free silicon-nanowire biosensors to detect cardiac troponin I for acute myocardial infarction diagnosis. *Biosens. Bioelectron.* **2012**, *34* (1), 267−272.
(157) Zhang, B.; Morales, A. W.; Peterson, R.; Tang, L.; Ye, J. Y. Label-free detection of cardiac troponin I with a photonic crystal biosensor. *Biosens. Bioelectron.* **2014**, *58*, 107−113.
(158) Kumbhat, S.; Shankaran, D. R.; Kim, S. J.; Gobi, K. V.; Joshi, V.; Miura, N. Surface plasmon resonance biosensor for dopamine using D3 dopamine receptor as a biorecognition molecule. *Biosens. Bioelectron.* **2007**, *23* (3), 421−427.
(159) Baron, R.; Zayats, M.; Willner, I. Dopamine-, L-DOPA-, adrenaline-, and noradrenaline-induced growth of Au nanoparticles: assays for the detection of neurotransmitters and of tyrosinase activity. *Anal. Chem.* **2005**, *77* (6), 1566−1571.
(160) Swamy, B. K.; Venton, B. J. Carbon nanotube-modified microelectrodes for simultaneous detection of dopamine and serotonin in vivo. *Analyst* **2007**, *132* (9), 876−884.
(161) Clark, J. J.; Sandberg, S. G.; Wanat, M. J.; Gan, J. O.; Horne, E. A.; Hart, A. S.; Akers, C. A.; Parker, J. G.; Willuhn, I.; Martinez, V.; et al. Chronic microsensors for longitudinal, subsecond dopamine detection in behaving animals. *Nat. Methods* **2010**, *7* (2), 126−129.
(162) Matsui, J.; Akamatsu, K.; Hara, N.; Miyoshi, D.; Nawafune, H.; Tamaki, K.; Sugimoto, N. SPR sensor chip for detection of small molecules using molecularly imprinted polymer with embedded gold nanoparticles. *Anal. Chem.* **2005**, *77* (13), 4282−4285.
(163) Chen, Z.; Zhang, C.; Zhou, T.; Ma, H. Gold nanoparticle based colorimetric probe for dopamine detection based on the interaction between dopamine and melamine. *Microchim. Acta* **2015**, *182* (5−6), 1003−1008.
(164) Wang, H.-B.; Zhang, H.-D.; Chen, Y.; Huang, K.-J.; Liu, Y.-M. A label-free and ultrasensitive fluorescent sensor for dopamine detection based on double-stranded DNA templated copper nanoparticles. *Sens. Actuators, B* **2015**, *220*, 146−153.
(165) Rand, E.; Periyakaruppan, A.; Tanaka, Z.; Zhang, D. A.; Marsh, M. P.; Andrews, R. J.; Lee, K. H.; Chen, B.; Meyyappan, M.; Koehne, J. E. A carbon nanofiber based biosensor for simultaneous detection of dopamine and serotonin in the presence of ascorbicacid. *Biosens. Bioelectron.* **2013**, *42*, 434−438.
(166) Jie, Y.; Wang, N.; Cao, X.; Xu, Y.; Li, T.; Zhang, X.; Wang, Z. L. Self-powered triboelectric nanosensor with poly (tetrafluoroethylene) nanoparticle arrays for dopamine detection. *ACS Nano* **2015**, *9* (8), 8376−8383.
(167) Han, H. S.; Ahmed, M. S.; Jeong, H.; Jeon, S. The determination of dopamine in presence of serotonin on dopamine-functionalized electrochemically prepared graphene biosensor. *J. Electrochem. Soc.* **2015**, *162* (4), B75−B82.
(168) Wang, P.; Xia, M.; Liang, O.; Sun, K.; Cipriano, A. F.; Schroeder, T.; Liu, H.; Xie, Y.-H. Label-free SERS selective detection of dopamine and serotonin using graphene-Au nanopyramid heterostructure. *Anal. Chem.* **2015**, *87* (20), 10255−10261.
(169) Wen, D.; Liu, W.; Herrmann, A. K.; Haubold, D.; Holzschuh, M.; Simon, F.; Eychmüller, A. Simple and Sensitive Colorimetric Detection of Dopamine Based on Assembly of Cyclodextrin - Modified Au Nanoparticles. *Small* **2016**, *12* (18), 2439−2442.
(170) Helle, M.; Boeije, L.; de Groot, E.; de Vos, A.; Aarden, L. Sensitive ELISA for interleukin-6: detection of IL-6 in biological fluids: synovial fluids and sera. *J. Immunol. Methods* **1991**, *138* (1), 47−56.
(171) Malhotra, R.; Patel, V.; Chikkaveeraiah, B. V.; Munge, B. S.; Cheong, S. C.; Zain, R. B.; Abraham, M. T.; Dey, D. K.; Gutkind, J. S.; Rusling, J. F. Ultrasensitive detection of cancer biomarkers in the clinic by use of a nanostructured microfluidic array. *Anal. Chem.* **2012**, *84* (14), 6249−6255.
(172) Huang, J.; Harvey, J.; Fam, W. D.; Nimmo, M. A.; Tok, I. A. Novel biosensor for Interleukin-6 detection. *Procedia Eng.* **2013**, *60*, 195−200.
(173) Fan, G.-C.; Ren, X.-L.; Zhu, C.; Zhang, J.-R.; Zhu, J.-J. A new signal amplification strategy of photoelectrochemical immunoassay for highly sensitive interleukin-6 detection based on TiO2/CdS/CdSe dual co-sensitized structure. *Biosens. Bioelectron.* **2014**, *59*, 45−53.
(174) Yoo, Y. K.; Lee, J.; Kim, J.; Kim, G.; Kim, S.; Kim, J.; Chun, H.; Lee, J. H.; Lee, C. J.; Hwang, K. S. Ultra-sensitive detection of brain-derived neurotrophic factor (BDNF) in the brain of freely moving mice using an interdigitated microelectrode (IME) biosensor. *Sci. Rep.* **2016**, *6*, 33694. (2016)

DOI: 10.1021/acssensors.8b00726
ACS Sens. 2018, 3, 2025−2044

(175) Tawa, K.; Satoh, M.; Uegaki, K.; Hara, T.; Kojima, M.; Kumanogoh, H.; Aota, H.; Yokota, Y.; Nakaoki, T.; Umetsu, M.; et al. Rapid and sensitive detection of brain-derived neurotrophic factor with a plasmonic chip. *Jpn. J. Appl. Phys.* **2013**, *52* (6S), 06GK01.
(176) Bockaj, M.; Fung, B.; Tsoulis, M.; Foster, L.; Soleymani, L. A Method for Electrochemical Detection of Brain Derived Neurotrophic Factor (BDNF) in plasma. *Anal. Chem.* **2018**, *90* (14), 8561−8566.
(177) Xu, H.; Luo, J.; Wang, Y.; Song, Y.; Wang, L.; Cai, X. In *Label-free electrochemical detection of brain-derived neurotrophic factor based on a novel immune microelectrode array*; 2017 IEEE 17th International Conference on Nanotechnology (IEEE-NANO); IEEE: 2017; pp 584−589.
(178) Murdock, R. C.; Shen, L.; Griffin, D. K.; Kelley-Loughnane, N.; Papautsky, I.; Hagen, J. A. Optimization of a paper-based ELISA for a human performance biomarker. *Anal. Chem.* **2013**, *85* (23), 11634−11642.
(179) Sanghavi, B. J.; Varhue, W.; Chávez, J. L.; Chou, C.-F.; Swami, N. S. Electrokinetic preconcentration and detection of neuropeptides at patterned graphene-modified electrodes in a nanochannel. *Anal. Chem.* **2014**, *86* (9), 4120−4125.
(180) Fernandez, R. E.; Sanghavi, B. J.; Farmehini, V.; Chávez, J. L.; Hagen, J.; Kelley-Loughnane, N.; Chou, C.-F.; Swami, N. S. Aptamer-functionalized graphene-gold nanocomposites for label-free detection of dielectrophoretic-enriched neuropeptide Y. *Electrochem. Commun.* **2016**, *72*, 144−147.
(181) Arya, S. K.; Chornokur, G.; Venugopal, M.; Bhansali, S. Dithiobis (succinimidyl propionate) modified gold microarray electrode based electrochemical immunosensor for ultrasensitive detection of cortisol. *Biosens. Bioelectron.* **2010**, *25* (10), 2296−2301.
(182) Homola, J. Surface Plasmon Resonance Sensors for Detection of Chemical and Biological Species. *Chem. Rev.* **2008**, *108* (2), 462−493.
(183) Krejcova, L.; Michalek, P.; Rodrigo, M. M.; Heger, Z.; Krizkova, S.; Vaculovicova, M.; Hynek, D.; Adam, V.; Kizek, R. Nanoscale virus biosensors: state of the art. *Nanobiosens. Dis. Diagn.* **2015**, *4*, 47−66.
(184) Hu, J.; Wang, S.; Wang, L.; Li, F.; Pingguan-Murphy, B.; Lu, T. J.; Xu, F. Advances in paper-based point-of-care diagnostics. *Biosens. Bioelectron.* **2014**, *54*, 585−597.
(185) Alim, S.; Vejayan, J.; Yusoff, M. M.; Kafi, A. Recent Uses of Carbon nanotubes & Gold nanoparticles in Electrochemistry with application in Biosensing: A review. *Biosens. Bioelectron.* **2018**, *121*, 125−136.
(186) Kim, K. S.; Lee, H.-S.; Yang, J.-A.; Jo, M.-H.; Hahn, S. K. The fabrication, characterization and application of aptamer-functionalized Si-nanowire FET biosensors. *Nanotechnology* **2009**, *20* (23), 235501.
(187) Dzyadevych, S. V.; Soldatkin, A. P.; El'skaya, A. V.; Martelet, C.; Jaffrezic-Renault, N. Enzyme biosensors based on ion-selective field-effect transistors. *Anal. Chim. Acta* **2006**, *568* (1−2), 248−258.
(188) Lee, C.-S.; Kim, S. K.; Kim, M. Ion-sensitive field-effect transistor for biological sensing. *Sensors* **2009**, *9* (9), 7111−7131.
(189) Yuqing, M.; Jianguo, G.; Jianrong, C. Ion sensitive field effect transducer-based biosensors. *Biotechnol. Adv.* **2003**, *21* (6), 527−534.
(190) Elghanian, R.; Storhoff, J. J.; Mucic, R. C.; Letsinger, R. L.; Mirkin, C. A. Selective colorimetric detection of polynucleotides based on the distance-dependent optical properties of gold nanoparticles. *Science* **1997**, *277* (5329), 1078−1081.
(191) Liu, J.; Lu, Y. Fast colorimetric sensing of adenosine and cocaine based on a general sensor design involving aptamers and nanoparticles. *Angew. Chem.* **2006**, *118* (1), 96−100.
(192) Ou, L.-J.; Jin, P.-Y.; Chu, X.; Jiang, J.-H.; Yu, R.-Q. Sensitive and visual detection of sequence-specific DNA-binding protein via a gold nanoparticle-based colorimetric biosensor. *Anal. Chem.* **2010**, *82* (14), 6015−6024.
(193) Daniel, M.-C.; Astruc, D. Gold nanoparticles: assembly, supramolecular chemistry, quantum-size-related properties, and applications toward biology, catalysis, and nanotechnology. *Chem. Rev.* **2004**, *104* (1), 293−346.
(194) Treguer-Delapierre, M.; Majimel, J.; Mornet, S.; Duguet, E.; Ravaine, S. Synthesis of non-spherical gold nanoparticles. *Gold Bull.* **2008**, *41* (2), 195−207.
(195) Cao, J.; Sun, T.; Grattan, K. T. Gold nanorod-based localized surface plasmon resonance biosensors: A review. *Sens. Actuators, B* **2014**, *195*, 332−351.
(196) Liu, J.; Lu, Y. Fast colorimetric sensing of adenosine and cocaine based on a general sensor design involving aptamers and nanoparticles. *Angew. Chem., Int. Ed.* **2006**, *45* (1), 90−94.
(197) Zhao, W.; Brook, M. A.; Li, Y. Design of gold nanoparticle -based colorimetric biosensing assays. *ChemBioChem* **2008**, *9* (15), 2363−2371.
(198) Lee, L. G.; Nordman, E. S.; Johnson, M. D.; Oldham, M. F. A low-cost, high-performance system for fluorescence lateral flow assays. *Biosensors* **2013**, *3* (4), 360−373.
(199) Dodeigne, C.; Thunus, L.; Lejeune, R. Chemiluminescence as diagnostic tool. A review. *Talanta* **2000**, *51* (3), 415−439.
(200) Roda, A.; Mirasoli, M.; Guardigli, M.; Michelini, E.; Simoni, P.; Magliulo, M. Development and validation of a sensitive and fast chemiluminescent enzyme immunoassay for the detection of genetically modified maize. *Anal. Bioanal. Chem.* **2006**, *384* (6), 1269−1275.
(201) Roda, A.; Mirasoli, M.; Michelini, E.; Di Fusco, M.; Zangheri, M.; Cevenini, L.; Roda, B.; Simoni, P. Progress in chemical luminescence-based biosensors: a critical review. *Biosens. Bioelectron.* **2016**, *76*, 164−179.
(202) Willner, I.; Katz, E. Magnetic control of electrocatalytic and bioelectrocatalytic processes. *Angew. Chem., Int. Ed.* **2003**, *42* (38), 4576−4588.
(203) Vabbina, P. K.; Kaushik, A.; Pokhrel, N.; Bhansali, S.; Pala, N. Electrochemical cortisol immunosensors based on sonochemically synthesized zinc oxide 1D nanorods and 2D nanoflakes. *Biosens. Bioelectron.* **2015**, *63*, 124−130.
(204) Willets, K. A.; Van Duyne, R. P. Localized surface plasmon resonance spectroscopy and sensing. *Annu. Rev. Phys. Chem.* **2007**, *58*, 267−297.
(205) Turner, A. P. Biosensors: sense and sensibility. *Chem. Soc. Rev.* **2013**, *42* (8), 3184−3196.
(206) Saha, K.; Agasti, S. S.; Kim, C.; Li, X.; Rotello, V. M. Gold nanoparticles in chemical and biological sensing. *Chem. Rev.* **2012**, *112* (5), 2739−2779.

DOI: 10.1021/acssensors.8b00726
ACS Sens. 2018, 3, 2025−2044

Supplementary Information

DOI: 10.1021/acssensors.8b00726

Stress Biomarkers in Biological Fluids and Their Point-of-Use Detection

Andrew J. Steckl* and Prajokta Ray

Nanoelectronics Laboratory, University of Cincinnati, Cincinnati OH 45221-0030, United States

* a.steckl@uc.edu

Expanded Table 4

Summary of publication highlights of cortisol, troponin, dopamine, IL-6 NPY, and BDNF biosensing (with list of materials, biosensor substrate, components and equipment utilized).

Biofluid	LOD	Detection Mechanism	Substrate	Components	Ref
Cortisol					
Saliva	1pM - 10 nM	Immuno-EC impedance	Si	1. Dithiobis (succinimidyl propionate) 2. Sodium borohydride 3. Monoclonal cortisol antibody 4. Hydrocortisone 5. Bio electrodes (EA-Gly/C-Mab/DTSP/IDμE) 6. Si wafer	1
Saliva	0.3 – 60 ng/mL	Immunoassay-coupled with chemiluminescence	LFIA	1. Cortisol standard 2. Polyclonal anti-horseradish peroxidase (hrp) antibody 3. Polyclonal anti-cortisol antibody 4. HRP–conjugate cortisol 5. Salivettes cotton swabs 6. LFA strips 7. Elisa chemiluminescent substrate for hrp	2
Saliva Serum	LOD:10 pg/mL	Aptamer-AuNP based EC detection	Nano slit device in quartz	1. Graphene-modified glassy carbon electrodes 2. Graphene oxide 3. SU-8 4. Ag/AgCl electrode 5. Polysilsesquioxane (PSQ) 6. $HAuCl_4$ 7. Sodium citrate 8. Cortisol aptamer 9. Ethyl acetate 10. Triamcinolone 11. Amicon ultrafilters 12. Elisa kit 13. Radioimmunoassay kit 14. Graphite powder	3
Serum	10-80 μM	Au nanowire-based EC detection coupled with immunoassay	Si	1. Cortisone 2. Hydrocortisone 3. Anti-cortisol ab 4. 3α-hydroxysteroid dehydrogenase 5. 1-Ethyl-3-[3-dimethylaminopropyl] carbodiimide hydrochloride 6. EZ-link sulfo-NHS-LC-biotin 7. Strepatavidin 8. DL-thioctic acid 9. Modified gold (Au) nanowires 10. Ag/AgCl 11. Pt 12. Silicon chip	4

Plasma Saliva Urine	pg/mL range	EC luminescence immunoassay, immunochemiluminescent assay	Commercial ECLIA and ICLA kit	1. ECLIA kit (Roche) 2. ICLIA kit (Diasorin) 3. Urine collection 4. Saliva collection 5. Plasma collection	5
Saliva	0.36 ng/mL (buffer) 1 ng/mL (saliva)	SPR coupled with immunoassay	Spreeta sensor chip (Texas Instr.)	1. Spreeta 2000 sensor chip 2. Cortisol conjugated BSA 3. Monoclonal anti cortisol antibody 4. Salivette cotton swabs 5. Aminolink plus immobilization kit 6. Salivary cortisol enzyme immunoassay kit 7. Hydrophillic hollow fiber (minntech) flow cell	6
Saliva	0.1 – 10 ng/mL	EC immunoassay with fluid control design for on-chip pretreatment of saliva sample for testing	SAM polymer, glass substrate	1. Monoclonal anti-cortisol antibody 2. Cortisol-21-hemisuccinate 3. Glucose oxidase 4. Sulfuric acid 5. Hydrogen peroxide 6. 5-carboxy-1-pentanethiol 7. *N*-hydroxysulfosuccinimide 8. 1-ethy1-3-carbodiimide 9. Cortisol standard 10. Pt electrodes (WE, CE, RE)	7
Sweat, Saliva	0.1 ng/mL (cortisol) 0.1 mM lactate	electrochemical chronoamperometric detection	Graphene	1. Graphene oxide 2. N-hydroxysuccinimide 3. N-(3-dimethylaminopropyl)-N'-ethylcarbodiimide hydrochloride (EDC) 4. Cortisol 5. Uric acid 6. D(+) glucose 7. L-(+)-lactic acid 8. L-ascorbic acid 9. $K_3[Fe(CN)_6]$ 10. $K_4[Fe(CN)_6]$ 11. Anti-cortisol antibody 12. Anti-lactate dehydrogenase 13. Artificial sweat and saliva 14. Carbon screen-printed electrodes 15. Ag/AgCl	8
Sweat	1 pg/mL (synthetic sweat); 1 ng/mL (human sweat; range 10 - 200 ng/mL)	Electric Double Layer modulated biosensing	ZnO on Parylene	1. Polyamide substrates 2. Dithiobis [succinimidyl propionate] 3. Dimethyl sulfoxide (DMSO) 4. α -cortisol antibody 5. Cortisol hormone 6. IL-1β antigen 7. Parylene C 8. ZnO thin film deposited 16. Gold electrode	9

Biofluid	LOD	Detection Mechanism	Substrate	Components	Ref
Troponin					
Buffer	1 – 100 ng/mL	EC detection of anti-troponin and troponin interaction on conducting paper using aniline polymerization on screen-printed paper electrode	Conducting paper substrate	1. Whatman filter paper 2. Aniline 3. Graphite, silver powder (conductive ink) 4. Electro polymerization and electro-chemical characterization 5. SPPE (WE), Pt (AE), Ag/AgCl (RE) 6. $[Fe(CN)_6]^{3-/4-}$.	10
Plasma	0.03 – 6.5 ng/mL	Optomagnetic biosensor – sandwich immunoassay performed on stationary liquid assay	Plastic disposable substrate	1. Superparamagnetic particles functionalized with carboxylic acid group 2. Antibody pairs recognizing various epitopes on cTnI 3. Monoclonal antibody A34780359P 4. Goat polyclonal capture antibody 5. Human troponin complex	11
Serum	0.01 – 5 ng/mL (PBS); 0.07 – 6.9 ng/mL (human serum)	Capacitive biosensor coupled with immunoassay	Si	1. Lyophilized human troponin T 2. Monoclonal goat anti-human tnt 3. 2-Aminoethanothiol 4. 25% Glutaraldehyde 5. Glycine 6. Al electrode deposited on Si. 7. Si <100> wafer	12
Buffer	0.092 – 46 ng/mL	SiNW based FET sensor responsive towards interaction between immobilized troponin antibody and protein	si	1. SOI wafers (6 in., p-type (1 0 0), _: 10–20 _ cm) 2. Aldehyde 3. (3-aminopropyl)triethoxysilane (APTES), 4. Glutaraldehyde 5. Ethanolamine 6. Phosphate buffered saline, BSA 7. TMAH, 99.9999%) 8. CTnI protein 9. Monoclonal antibody	13
Plasma	0.1 ng/mL	(PC-TIR) Photonic Crystal Total Internal Reflection	PC-TIR sensor chip on PDMS substrate	1. 5-layer PC using Titania, Silica, Silcon 2. PDMS 3. 3-Aminopropyltriethoxysilane 4. CTnI antibodies. 5. Carboxylmethylated (CM) Dextran 6. 2-(N-morpholino)ethanesulfonic acid 7. 1-Ethyl-3(3-dimethyl amino-propyl) carbodiimide 8. N-hydroxysuccinimide 9. Lyophilized human plasma 10. 3.8% Trisodium citrate	14

Biofluid	LOD	Detection Mechanism	Substrate	Components	Ref
Dopamine					
Buffer (PBS)	0.085 to 700 ng/mL	SPR using D3 dopamine receptor as recognition element (SPR coupled with immunoassay)	Au sputtered on Si substrate	1. D3 dopamine receptor 2. Dopamine hydrochloride 3. N-Hydroxisuccinide 4. Dicyclohexicarboximide 5. 3,4 dihydroxyphenol acetic acid 6. DOPA alanine 7. Ascorbic acid 8. Template stripped gold slides	15
Buffer	2.5 µM	Colorimetric detection, plasmon absorbance of Au-NP mediated by exposure of dopamine, adrenaline, NE	Solution test, in vial	1. Cetyltrimethylammonium chloride 2. Dopamine, l-dopa, adrenaline, noradrenaline 3. Hydrogen tetrachloroaurate 4. L-tyrosine 5. Tyrosinase	16
Buffer In vivo (corpus striatum of rat)	1 – 5 µM (dopamine and serotonin)	Electrochemical detection of CNT coated carbon fiber microelectrode for simultaneous detection of dopamine and serotonin (in vivo)	Soln. phase In vivo electrode implant	1. Dopamine & serotonin hydrochloride 2. Carbon-fiber microelectrodes 3. Electrode responses to fast concentration changes tested using stainless steel HPLC loop flow injector 4. Single-walled carbon nanotubes 5. HNO_3 6. Nafion	17
In vivo (rats)	Physiol. range (sensor responds to dopamine release in vivo)	Voltammetry microsensor	Carbon fiber in polyimide covered fused-silica capillary	1. Single carbon fiber 2. Fused silica 3. 2-propanol 4. Devcon two-component epoxy 5. Silver connector	18
Buffer	10 µM	SPR sensor chip (Au – film: Molecular imprinted polymer gel; AuNP immobilized MI polymer gel)	Polymer gel imprinted on Au sputtered glass	1. Dopamine 2. Acrylic acid 3. 2,2′-azobis (2,4dimethlvarelonitrile) 4. N-isopropylacrylamide 5. N,n′-methylenbisacrylamide (bis) 6. Tetraoctylammonium bromide 7. Hydrogen tetrachloroaurat 8. Allyl mercaptan 9. Decanethiol 10. 11-Mercaptoundecanoic acid 11. Sodium borohydride 12. Au-sputtered cover glass	19
Buffer	33nM – 3.33 mM	Colorimetric detection – AuNP-DA interaction in presence of melamine	Quartz Cuvette	1. Chloroauric acid trihydrate 2. Sodium citrate 3. Melamine 4. Dopamine hydrochloride 5. Tris base	20

Buffer	20pM Range: 0.1–10,000 nM	Fluorescence intensity (ds-DNA and CuNP) quenching with increasing dopamine concentration	Quartz fluorescence cell	1. Dopamine hydrochloride 2. $CuSO_4 \cdot 5H_2O$ 3. Ascorbic acid 4. MOPS buffer 5. DNA templates	21
Buffer	50 nM for DA; 250 nM for 5-HT.	Dynamic pulse voltametric sensing of DA, HT in AA	CnF on Si substrate	1. CNF grown on Si substrate 2. AgCl electrode 3. Nitric acid 4. DA (5-hydroxytyramine) 5. 5-HT (5-hydroxytryptamine) 6. Tris buffer 7. Ascorbic acid	22
Buffer	0.5 µM (Linear range: 10 µM to 1 mM)	Self-powered triboelectric nanosensing	PMMA	1. PMMA 2. PTFE 3. Aluminum 4. Trishydroxymethylaminomethane 5. DA hydrochloride 6. AA, and UA solutions 7. Phosphate 8. Au deposition	23
Serum	0.04 µM (Linear range 0.5–100 µM)	Electrochemical Detection	Graphene	1. Graphite powder 2. 5-HT 3. DA 4. Glucose 5. Ascorbic acid 6. H_2O_2 7. Uric acid (UA) 8. *N, N*-dimethylformamide 9. toluene, chloroform, hexane 10. NaH_2PO_4, NaOH, H_3PO4. 11. Ag/AgCl, Pt 12. H_2SO_4:H_3PO_4 13. $KMnO_4$ 14. Alumina paste	24
Buffer Cell culture media Simulated body fluids	0.1 nM	SERS	Si/SiO_2	1. Si wafer 2. Polystyrene (PS) nanospheres 3. SiO_2/Si 4. Ethanol. 5. Piranha soln. 6. Cr film 7. HF solution 8. Monolayer graphene 9. PMMA 10. $CuCl_2$	25
Serum CSF	20 nM	Colorimetric detection using modified AuNP	Solution processing	1. Chloroauric acid 2. Sodium borohydride 3. Natural beta-CD. 4. Dopamine 5. Buffer 6. a-CSF 7. Human serum 8. Glucose 9. Lactic acid 10. Ascorbic acid 11. Uric acid 12. 2-phenylethylaminepyrocatechol)	26

Biofluid	LOD	Detection Mechanism	Substrate	Components	Ref
IL-6					
Serum, Synovial fluid	1 pg/mL	ELISA	Microtiter plate	1. Il-6 2. Monoclonal anti il-6 ab 3. ELISA	27
Serum (calf)	0.5 pg/mL	EC immune-sensing (CNT based)	Basal plane pyrolytic graphite disks	1. Monoclonal antihuman IL-6 antibody 2. Biotinylated antihuman IL-6 antibody 3. Recombinant human IL-6 in calf serum 4. Streptavidin-horseradish peroxidase (HRP) 5. Single-walled carbon nanotubes 6. Carboxylated multiwalled carbon nanotubes	28
Serum (human)	IL-6 5 fg/mL; IL-8 10 fg/mL	EC immunosensing detection	PDMS	1. Microfluidic device fabricated on PDMS 2. Antibodies for IL-6, IL-8, VEGF, and VEGF-C 3. Protein standards 4. Biotinylated horseradish peroxidase 5. Streptavidin-coated magnetic beads 6. Immortalized HaCat cells 7. Oral keratinocyte cells 8. Oral cancer cell lines 9. Glutathione-decorated AuNps 10. Poly(diallydimethylammonium chloride) (PDDA) 11. 1-[3-(Dimethylamino)- propyl]-3-ethylcarbodiimide hydrochloride (EDC) 12. N-hydroxysulfosuccinimide (NHSS) solutions	29
Buffer	4.7 pg/mL	Graphene Oxide-based amperometric Field Effect Transistor (FET) sensing	SiO_2	1. Graphite flakes 2. IL-6 protein and antibody 3. H_2SO_4, $KMnO_4$, H_2O_2 4. Silicon dioxide chips 5. 1-Pyrenebutanoic acid 6. Succinimidyl ester (PBSE) linker	30
Buffer	0.38 pg/mL (range 1 pg/mL – 100 ng/mL)	Photoelectrochemical Immunoassay	ITO	1. TiO_2 powder 2. Cadmium nitrate 3. Sodium sulfide, methanol 4. Cadmium chloride 5. Sodium hydroxide 6. Selenium powder 7. Sodium borohydride 8. Thiolglycolic acid 9. Chitosan powder 10. 1-Ethyl-3-(3-dimethylaminopropyl) car-bodiimide hydrochloride (EDC) 11. Ascorbic acid 12. Glutaraldehyde 13. Anti-IL-6 14. Human IL-6 15. Human Interleukin-8 16. Carcinoembryonic antigen 17. Prostate- specific antigen(PSA) 18. Human IgG	31

Biofluid	LOD	Detection Mechanism	Substrate	Components	Ref
			NPY		
Buffer Saliva	10 pM range	ELISA (AuNP enhanced)	Paper	1. NPY 2. Rabbit Igg 3. Goat anti-rabbit igg conjugated with alkaline phosphate 4. Goat anti-rabbit igg 5. P-nitrophenyl phosphate 6. Mouse anti-human npy monoclonal antibody 7. 1-Step ultra tmbelisa 8. Supersignal elisa pico chemiluminescent substrate 9. Quantablu fluorogenic peroxidase substrate k 10. Ap and horseradish peroxidase (hrp) lightning link enzyme labeling kit 11. Thiol- and carboxyl modified poly(ethylene glycol)	32
Buffer	pM level from sub nanoliter sample	EC detection coupled with electrokinetic sample pre-concentration	Microfluidic chip on quartz substrate bonded to glass coverslip	1. Fluorescently labeled NPY 2. Orexin A 3. Quartz substrate 4. Glassy carbon electrode (GCE) 5. Graphene oxide 6. Nafion 7. $HAuCl_4$ 8. Ag/AgCl reference	33
Buffer	10 pM	Aptamer functionalized NPY detection	COC polymer	1. NPY aptamer 2. 6-mercapto-1 hexanol 3. Buffer 4. Pristine graphite 5. N-heptane 6. Exfoliated graphene sheets 7. Cyclic olefin copolymer 8. Shipley Microposit S1813 9. $HAuCl_4$, HF 10. MCH solution 11. Ag/AgCl, Pt electrodes 12. NPY	34

Biofluid	LOD	Detection Mechanism	Substrate	Components	Ref
BDNF					
Buffer CSF	pg/mL BDNF sensitivity	Impedance measurement - interaction of BDNF and BDNF antibody immobilized on electrode surface.	Biosensor chip (Pt/Ti electrode system fabricated on Si/SiO_2 coupled with PDMS microfluidic channel)	1. Si wafer, with SiO_2 deposition 2. Pt/Ti electrode (deposited and patterned on Si/SiO_2) 3. PDMS chip (microfluidic channel) 4. 3-(ethoxydimethylsilyl) propylamine solution 5. Polyvinyl pyrrolidone-aldehyde solution 6. Sodium borohydride 7. Glutaraldehyde solution 8. Bdnf antibody 9. Recombinant bdnf 10. Artificial cerebrospinal fluid	35
Serum	5–7 ng/mL	SPR sensor chip	SiO2	1. SiO2 2. ZnO 3. Cr, Ag deposited 4. Biotinylated-anti-ZnO antibody 5. Cover glass 6. BDNF propeptide 7. Cy5-labeled anti-BDNF antibody	36
Plasma	0.1 – 2 ng/mL	Electrochemical – immunosensing	polysterene (PS) substrate	1. BDNF antigen and anti BDNF antibody 2. Gold chloride (HAuCl) 3. 50% (w/w) glutaraldehyde 4. Potassium ferricyanide (FiCN, 99.0%) 5. Cystamine 6. Potassium chloride (KCl, ≥99.0%) 7. Phosphate buffered solution 8. Sulfuric acid (H2SO4, 98%) 9. 2-Propanol (99.5%) 10. Immobilized tris(2-carboxyethyl) phosphine (TCEP) 11. Tris- (hydroxymethyl)aminomethane (tris, ≥99.9%) 12. Hydrogen peroxide (H2O2) 13. Polysterene (PS) substrate	37
Serum	5 pg/mL (linear range 0.01 – 100 ng/mL)	Electrochemical – immunosensing	Glass	1. Thionine (THI) 2. PBS 3. Dopamine 4. Multiwalled CNT 5. AA, Uric Acid 6. BSA 7. Chitosan 8. D Glucose 9. BDNF ELISA 10. Human hemoglobin 11. BDNF 12. Anti BDNF 13. Human serum samples 14. Ag/AgCl	38

References:

1. Arya, S. K.; Chornokur, G.; Venugopal, M.; Bhansali, S., Antibody functionalized interdigitated μ-electrode (IDμE) based impedimetric cortisol biosensor. *Analyst* **2010,** *135* (8), 1941-1946.
2. Zangheri, M.; Cevenini, L.; Anfossi, L.; Baggiani, C.; Simoni, P.; Di Nardo, F.; Roda, A., A simple and compact smartphone accessory for quantitative chemiluminescence-based lateral flow immunoassay for salivary cortisol detection. *Biosensors and Bioelectronics* **2015,** *64*, 63-68.
3. Sanghavi, B. J.; Moore, J. A.; Chávez, J. L.; Hagen, J. A.; Kelley-Loughnane, N.; Chou, C.-F.; Swami, N. S., Aptamer-functionalized nanoparticles for surface immobilization-free electrochemical detection of cortisol in a microfluidic device. *Biosensors and Bioelectronics* **2016,** *78*, 244-252.
4. Kumar, A.; Aravamudhan, S.; Gordic, M.; Bhansali, S.; Mohapatra, S. S., Ultrasensitive detection of cortisol with enzyme fragment complementation technology using functionalized nanowire. *Biosensors and Bioelectronics* **2007,** *22* (9-10), 2138-2144.
5. Carrozza, C.; Corsello, S. M.; Paragliola, R. M.; Ingraudo, F.; Palumbo, S.; Locantore, P.; Sferrazza, A.; Pontecorvi, A.; Zuppi, C., Clinical accuracy of midnight salivary cortisol measured by automated electrochemiluminescence immunoassay method in Cushing's syndrome. *Annals of Clinical Biochemistry* **2010,** *47* (3), 228-232.
6. Stevens, R. C.; Soelberg, S. D.; Near, S.; Furlong, C. E., Detection of cortisol in saliva with a flow-filtered, portable surface plasmon resonance biosensor system. *Analytical Chemistry* **2008,** *80* (17), 6747-6751.
7. Yamaguchi, M.; Matsuda, Y.; Sasaki, S.; Sasaki, M.; Kadoma, Y.; Imai, Y.; Niwa, D.; Shetty, V., Immunosensor with fluid control mechanism for salivary cortisol analysis. *Biosensors and Bioelectronics* **2013,** *41*, 186-191.
8. Tuteja, S. K.; Ormsby, C.; Neethirajan, S., Noninvasive Label-Free Detection of Cortisol and Lactate Using Graphene Embedded Screen-Printed Electrode. *Nano-Micro Letters* **2018,** *10* (3), 41. DOI: https://doi.org/10.1007/s40820-018-0193-5
9. Munje, R. D.; Muthukumar, S.; Selvam, A. P.; Prasad, S., Flexible nanoporous tunable electrical double layer biosensors for sweat diagnostics. *Scientific Reports* **2015,** *5*, 14586. DOI: https://doi.org/10.1038/srep14586
10. Jagadeesan, K. K.; Kumar, S.; Sumana, G., Application of conducting paper for selective detection of troponin. *Electrochemistry Communications* **2012,** *20*, 71-74.
11. Dittmer, W. U.; Evers, T. H.; Hardeman, W. M.; Huijnen, W.; Kamps, R.; de Kievit, P.; Neijzen, J. H.; Nieuwenhuis, J. H.; Sijbers, M. J.; Dekkers, D. W., Rapid, high sensitivity, point-of-care test for cardiac troponin based on optomagnetic biosensor. *Clinica Chimica Acta* **2010,** *411* (11-12), 868-873.
12. de Vasconcelos, E. A.; Peres, N. G.; Pereira, C. O.; da Silva, V. L.; da Silva Jr, E. F.; Dutra, R. F., Potential of a simplified measurement scheme and device structure for a low cost label-free point-of-care capacitive biosensor. *Biosensors and Bioelectronics* **2009,** *25* (4), 870-876.
13. Kong, T.; Su, R.; Zhang, B.; Zhang, Q.; Cheng, G., CMOS-compatible, label-free silicon-nanowire biosensors to detect cardiac troponin I for acute myocardial infarction diagnosis. *Biosensors and Bioelectronics* **2012,** *34* (1), 267-272.
14. Zhang, B.; Morales, A. W.; Peterson, R.; Tang, L.; Ye, J. Y., Label-free detection of cardiac troponin I with a photonic crystal biosensor. *Biosensors and Bioelectronics* **2014,** *58*, 107-113.
15. Kumbhat, S.; Shankaran, D. R.; Kim, S. J.; Gobi, K. V.; Joshi, V.; Miura, N., Surface plasmon resonance biosensor for dopamine using D3 dopamine receptor as a biorecognition molecule. *Biosensors and Bioelectronics* **2007,** *23* (3), 421-427.
16. Baron, R.; Zayats, M.; Willner, I., Dopamine-, L-DOPA-, adrenaline-, and noradrenaline-induced growth of Au nanoparticles: assays for the detection of neurotransmitters and of tyrosinase activity. *Analytical Chemistry* **2005,** *77* (6), 1566-1571.
17. Swamy, B. K.; Venton, B. J., Carbon nanotube-modified microelectrodes for simultaneous detection of dopamine and serotonin in vivo. *Analyst* **2007,** *132* (9), 876-884.
18. Clark, J. J.; Sandberg, S. G.; Wanat, M. J.; Gan, J. O.; Horne, E. A.; Hart, A. S.; Akers, C. A.; Parker, J. G.; Willuhn, I.; Martinez, V., Chronic microsensors for longitudinal, subsecond dopamine detection in behaving animals. *Nature Methods* **2010,** *7* (2), 126.

19. Matsui, J.; Akamatsu, K.; Hara, N.; Miyoshi, D.; Nawafune, H.; Tamaki, K.; Sugimoto, N., SPR sensor chip for detection of small molecules using molecularly imprinted polymer with embedded gold nanoparticles. *Analytical Chemistry* **2005,** *77* (13), 4282-4285.
20. Chen, Z.; Zhang, C.; Zhou, T.; Ma, H., Gold nanoparticle based colorimetric probe for dopamine detection based on the interaction between dopamine and melamine. *Microchimica Acta* **2015,** *182* (5-6), 1003-1008.
21. Wang, H.-B.; Zhang, H.-D.; Chen, Y.; Huang, K.-J.; Liu, Y.-M., A label-free and ultrasensitive fluorescent sensor for dopamine detection based on double-stranded DNA templated copper nanoparticles. *Sensors and Actuators B: Chemical* **2015,** *220*, 146-153.
22. Rand, E.; Periyakaruppan, A.; Tanaka, Z.; Zhang, D. A.; Marsh, M. P.; Andrews, R. J.; Lee, K. H.; Chen, B.; Meyyappan, M.; Koehne, J. E., A carbon nanofiber based biosensor for simultaneous detection of dopamine and serotonin in the presence of ascorbicacid. *Biosensors and Bioelectronics* **2013,** *42*, 434-438.
23. Jie, Y.; Wang, N.; Cao, X.; Xu, Y.; Li, T.; Zhang, X.; Wang, Z. L., Self-powered triboelectric nanosensor with poly (tetrafluoroethylene) nanoparticle arrays for dopamine detection. *ACS nano* **2015,** *9* (8), 8376-8383.
24. Han, H. S.; Ahmed, M. S.; Jeong, H.; Jeon, S., The determination of dopamine in presence of serotonin on dopamine-functionalized electrochemically prepared graphene biosensor. *Journal of The Electrochemical Society* **2015,** *162* (4), B75-B82.
25. Wang, P.; Xia, M.; Liang, O.; Sun, K.; Cipriano, A. F.; Schroeder, T.; Liu, H.; Xie, Y.-H., Label-free SERS selective detection of dopamine and serotonin using graphene-Au nanopyramid heterostructure. *Analytical chemistry* **2015,** *87* (20), 10255-10261.
26. Wen, D.; Liu, W.; Herrmann, A. K.; Haubold, D.; Holzschuh, M.; Simon, F.; Eychmüller, A., Simple and Sensitive Colorimetric Detection of Dopamine Based on Assembly of Cyclodextrin-Modified Au Nanoparticles. *Small* **2016,** *12* (18), 2439-2442.
27. Helle, M.; Boeije, L.; de Groot, E.; de Vos, A.; Aarden, L., Sensitive ELISA for interleukin-6: detection of IL-6 in biological fluids: synovial fluids and sera. *Journal of Immunological Methods* **1991,** *138* (1), 47-56.
28. Malhotra, R.; Patel, V.; Vaqué, J. P.; Gutkind, J. S.; Rusling, J. F., Ultrasensitive electrochemical immunosensor for oral cancer biomarker IL-6 using carbon nanotube forest electrodes and multilabel amplification. *Analytical Chemistry* **2010,** *82* (8), 3118-3123.
29. Malhotra, R.; Patel, V.; Chikkaveeraiah, B. V.; Munge, B. S.; Cheong, S. C.; Zain, R. B.; Abraham, M. T.; Dey, D. K.; Gutkind, J. S.; Rusling, J. F., Ultrasensitive detection of cancer biomarkers in the clinic by use of a nanostructured microfluidic array. *Analytical Chemistry* **2012,** *84* (14), 6249-6255.
30. Huang, J.; Harvey, J.; Fam, W. D.; Nimmo, M. A.; Tok, I. A., Novel biosensor for Interleukin-6 detection. *Procedia Engineering* **2013,** *60*, 195-200.
31. Fan, G.-C.; Ren, X.-L.; Zhu, C.; Zhang, J.-R.; Zhu, J.-J., A new signal amplification strategy of photoelectrochemical immunoassay for highly sensitive interleukin-6 detection based on TiO2/CdS/CdSe dual co-sensitized structure. *Biosensors and Bioelectronics* **2014,** *59*, 45-53.
32. Murdock, R. C.; Shen, L.; Griffin, D. K.; Kelley-Loughnane, N.; Papautsky, I.; Hagen, J. A., Optimization of a paper-based ELISA for a human performance biomarker. *Analytical Chemistry* **2013,** *85* (23), 11634-11642.
33. Sanghavi, B. J.; Varhue, W.; Chávez, J. L.; Chou, C.-F.; Swami, N. S., Electrokinetic preconcentration and detection of neuropeptides at patterned graphene-modified electrodes in a nanochannel. *Analytical Chemistry* **2014,** *86* (9), 4120-4125.
34. Fernandez, R. E.; Sanghavi, B. J.; Farmehini, V.; Chávez, J. L.; Hagen, J.; Kelley-Loughnane, N.; Chou, C.-F.; Swami, N. S., Aptamer-functionalized graphene-gold nanocomposites for label-free detection of dielectrophoretic-enriched neuropeptide Y. *Electrochemistry Communications* **2016,** *72*, 144-147.
35. Yoo, Y. K.; Lee, J.; Kim, J.; Kim, G.; Kim, S.; Kim, J.; Chun, H.; Lee, J. H.; Lee, C. J.; Hwang, K. S., Ultra-sensitive detection of brain-derived neurotrophic factor (BDNF) in the brain of freely moving mice using an interdigitated microelectrode (IME) biosensor. *Scientific Reports* **2016,** *6*, 33694. DOI: https://doi.org/10.1038/srep33694

36. Tawa, K.; Satoh, M.; Uegaki, K.; Hara, T.; Kojima, M.; Kumanogoh, H.; Aota, H.; Yokota, Y.; Nakaoki, T.; Umetsu, M., Rapid and sensitive detection of brain-derived neurotrophic factor with a plasmonic chip. *Japanese Journal of Applied Physics* **2013,** *52* (6S), 06GK01.
37. Bockaj, M.; Fung, B.; Tsoulis, M.; Foster, L.; Soleymani, L., A Method for Electrochemical Detection of Brain Derived Neurotrophic Factor (BDNF) in plasma. *Analytical Chemistry* **2018**. DOI: 10.1021/acs.analchem.8b01642
38. Xu, H.; Luo, J.; Wang, Y.; Song, Y.; Wang, L.; Cai, X. In *Label-free electrochemical detection of brain-derived neurotrophic factor based on a novel immune microelectrode array*, Nanotechnology (IEEE-NANO), 2017 IEEE 17th International Conference on, IEEE: 2017; pp 584-589.